Articles

A New Approach to Docking in the β_2-Adrenergic Receptor That Exploits the Domain Structure of G-Protein-Coupled Receptors

Paul R. Gouldson, Christopher R. Snell,† and Christopher A. Reynolds*

Department of Chemistry and Biological Chemistry, University of Essex, Wivenhoe Park, Colchester, Essex CO4 3SQ, United Kingdom, and Novartis Institute for Medical Sciences, 5 Gower Place, London WC1E 6BN, United Kingdom

Received September 13, 1996[⊗]

A novel technique for docking ligands to the β_2-adrenergic receptor is described which exploits the domain structure of this class of receptors. The ligands (norepinephrine, an agonist; pindolol, a partial agonist; and propranolol, an antagonist) were docked into the receptor using the key conserved aspartate on helix 3 (D^{113}) as an initial guide to the placement of the amino group and GRID maps (Goodford, P. J. *J. Med. Chem.* **1985,** *28*, 849) to identify the likely binding regions of the hydrophobic (and hydroxyl) moieties on the A domain (comprising of helices 1−5). The essence of the new approach involved pulling the B domain, which includes helices 6 and 7, away from the other domain by 5−7 Å. During the subsequent minimization and molecular dynamics, the receptor ligand complex reformed to yield structures which were very well supported by site-directed mutagenesis data. In particular, the model predicted a number of important interactions between the antagonist and key residues on helix 7 (notably Leu^{311} and Asn^{312}) which have not been described in many previous computer simulation studies. The justification for this new approach is discussed in terms of (a) phase space sampling and (b) mimicking the natural domain dynamics which may include domain swapping and dimerization to form a 5,6-domain-swapped dimer. The observed structural changes in the receptor when pindolol, the partial agonist, was docked were midway between those observed for propranolol and norepinephrine. These structural changes, particularly the changes in helix−helix interactions at the dimer interface, support the idea that the receptors have a very dynamic structure and may shed some light on the activation process. The receptor model used in these studies is well supported by experiment, including site-directed mutagenesis (helices 1−7), zinc binding studies (helices 2, 3, 5, and 6), the substituted cysteine accessibility method (helices 3, 5, and 7), and site-directed spin-labeling studies (helices 3−6).

Introduction

There is considerable interest in simulating the interaction of drugs with G-protein-coupled receptors, because this family of receptors[1,2] is an extremely important target in medicinal chemistry.[3] Docking is a central theme in receptor modeling, and here we wish to present a new strategy which is specific to this class of receptors. Finding the global minimum in protein−ligand interactions is not trivial, and in the G-protein-coupled receptors this problem may be exaggerated because the cavity within the apo receptor appears to be too small for its natural ligand. This small cavity size adversely affects phase space sampling, and this not only hampers the docking but may even result in erroneously high-energy receptor−ligand complexes. Consequently, our new approach to docking is designed to mimic the natural domain movement within the receptors. Our insights into the domain structure of G-protein-coupled receptors come mainly from the studies of Kobilka and Maggio which show that the two domains which include helices 1−5 and helices 6 and 7 can be coexpressed as separate unconnected domains without adversely affecting activity.[4,5] This new strategy for docking the drug is illustrated in Scheme 1.

Scheme 1. Schematic Diagram of the New Approach to Docking[a]

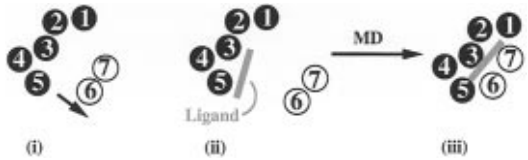

[a] In the first stage (i), helices 6 and 7 (the B domain shown in white) are pulled ∼7 Å away from the A domain. In the second stage (ii), the ligand (gray) is carefully docked into one of the two binding sites on the A domain (shown in black). In the final stage (iii), the complex is allowed to reform during a molecular dynamics simulation.

Here we are particularly interested in the docking process, but the lack of a three-dimensional structure adds an additional complication to this process. However, even if a crystal structure were available, problems would still arise in the modeling due to the dynamic nature of the structure which is apparent from the large structural changes induced by ligand binding[6,7] or a photon in rhodopsin[8] or in comparisons between wild type and constitutively active receptors.[9,10] Clearly, semiquantitative modeling would require crystal structures of many forms of the receptor, e.g., for the high- and low-affinity forms, but these are unlikely to be available in the foreseeable future. Despite these

† Novartis Institute for Medical Sciences.
⊗ Abstract published in *Advance ACS Abstracts,* October 1, 1997.

S0022-2623(96)00647-4 CCC: $14.00

Table 1. Sequences of the Transmembrane Segments Used To Build the Donnelly,[65] Bywater,[66] Hibert,[67] Lybrand,[39] and Current Models[a]

Helix 1----------	Helix 5----------
Current: VGMAILMSVIVLAIVFGNVLVITAIA	Rhodopsin: ..SFVIYMFVVHFIIPLIVIFFCYGQLVFTvkeaa
Donnelly: AWVGMAILMSVIVLAIVFGNVLVITAIAKFER	Current: AYAIASSIVSFYVPLVVMVFVYSRVFqvahrqlk
Bywater: WVGMAILMSVIVLAIVFGNVL	Donnelly: NQAYAIASSIVSFYVPLVVMVFVYSRVFQVALR
Lybrand: VGMAILMSVIVLAIVFGNVLVITAIAKFER	Bywater: IASSIVSFYVPLVVMVF
Hibert: VGMAILMSVIVLAIVFGNVLVIT	Lybrand: NQAYAIASSIVSFYVPLVVMVFVYSRVFQV
Helix 2----------	Hibert: AIASSIVSFYVPLVVMVFVYS
Current: NYFITSLACADLVMGLAVVPFGASHIL	Helix 6----------
Donnelly: NYFITSLACADLVMGLAVVPFGASHILMK	Rhodopsin: sattqkaekeVTRMVIIMVIAFLICWLPYAGVAFY...
Bywater: FITSLACADLVMGLAVVPFGASHI	Current: sskfckehkaLKTLGIIMGTFTLCWLPFFIVNIV
Lybrand: NYFITSLACADLVMGLAVVPFGASHILMKM	Donnelly: KEHKALKTLGIIMGTFTLCWLPFFIVNIV
Hibert: TSLACADLVMGLAVVPFGASHIL	Bywater: LKTLGIIMGTFTLCWLPFFIVNIV
Helix 3----------	Lybrand: HKALKTLGIIMGTFTLCWLPFFIVNIVHVI
Rhodopsin: ...NLEGFFATLGGEIALWSLVVLAIERyvvvc	Hibert: TLGIIMGTFTLCWLPFFIVNIV
Current: CEFWSIDVLCVTASIETLCVIAVDRY	Helix 7----------
Donnelly: FWCEFWSIDVLCVTASIETLCVIAVDRYVAI	Current: EVYILLNWLGYVNSAFNPLIYCrspdf
Bywater: EFWSIDVLCVTASIETLCVIAVDRY	Donnelly: IPKEVYILLNWLGYVNSAFNPLIYCRSPDFRIAF
Lybrand: CEFWSIDVLCVTASIETLCVIAVDRYVAI	Bywater: IPKEVYILLNWLGYVNSAFNPLIYC
Hibert: NFWCEFWSIDVLCVTASIET	Lybrand: KEVYILLNWLGYVNSAFNPLIYCRSPDFRI
Helix 4----------	Hibert: LIPKEVYILLNWLGYVNSAFNPLI
Rhodopsin: enhAIMGVAFTWVMALACAAPPLVGW...	
Current: KARVVILMVWIVSGLTSFLPIQMH	
Donnelly: TKNKARVVILMVWIVSGLTSFLPIQM	
Bywater: QSLLTKNKARVVILMVWIVSGLTSF	
Lybrand: TKNKARVVILMVWIVSGLTSFLPIQMHWYR	
Hibert: MVWIVSGLTSFLPIQM	

[a] The transmembrane helices in the current model lie between Val[34] and Ala[59] for helix 1, Asn[79] and Leu[95] for helix 2, Cys[106] and Tyr[132] for helix 3, Lys[149] and His[172] for helix 4; Ala[198] and Phe[223] for helix 5, Leu[272] and Val[297] for helix 6, and Glu[306] and Cys[227] for helix 7. The rhodopsin helical regions are also shown for helices 3−6; the bilayer/solvent boundary is marked by the switch form upper case to lower case.

factors, there are examples where careful modeling has made significant contributions (see, for example, ref 11), and these provide part of the impetus for developing methodologies to support further research in this area. Consequently, a new high-quality *model* of the β_2-adrenergic receptor (β_2-AR) will be presented, and this will be used to test whether the new docking approach can generate structures which are in agreement with site-directed mutagenesis and other experimental information[12,13] and which are stable during long molecular dynamics simulations.

Methods

The Receptor Model. The starting point for our model receptor structure was an earlier model[14] based on multiple sequence alignment and the bacteriorhodopsin template,[15] modified to conform to the projection structure of rhodopsin.[16−18] Following the lead of Pavel and Hubbard,[19] we have sought to improve the earlier model by incorporating as many experimental observations as possible. In particular, we used the following information to refine the previous model:

1. The transmembrane helix prediction algorithm of Sander[20] suggested that helix 7 originally had the wrong homology. The homology was shifted by eight residues (two turns) so that the top of helix 7 in the old model is now part of the extracellular loop connecting helices 6 and 7.

2. The transmembrane helix prediction algorithm[20] suggested that the intracellular end of helix 5 should be extended by eight residues (two extra turns). (The short length reflected its origins in an earlier model based on bacteriorhodopsin.) The solvent/bilayer boundary is now in good agreement with the site-directed spin-labeling studies on rhodopsin[21] (see Table 1) though these spin-labeling studies used micelles rather than lipid bilayers, and so perfect agreement should not be expected even though the spin-labeling results correspond reasonably well to those obtained from hydropathy considerations.[21,22]

3. Multiple sequence alignment[23] of rhodopsin with the β_1-, β_2-, and β_3-adrenergic receptors suggested that Ala[292] in rhodopsin, which is Asn[312] in the rat β_2-AR,[24] should point inward; helix 7 was twisted to account for this. Indeed,

Chart 1. Structures of the Ligands: (a) Epinephrine, an Agonist; (b) Propranolol, an Antagonist (or More Correctly an Inverse Agonist); (c) Pindolol; (d) IABP, a Photoaffinity Ligand; and (e) ICYP-da, a Photoaffinity Ligand

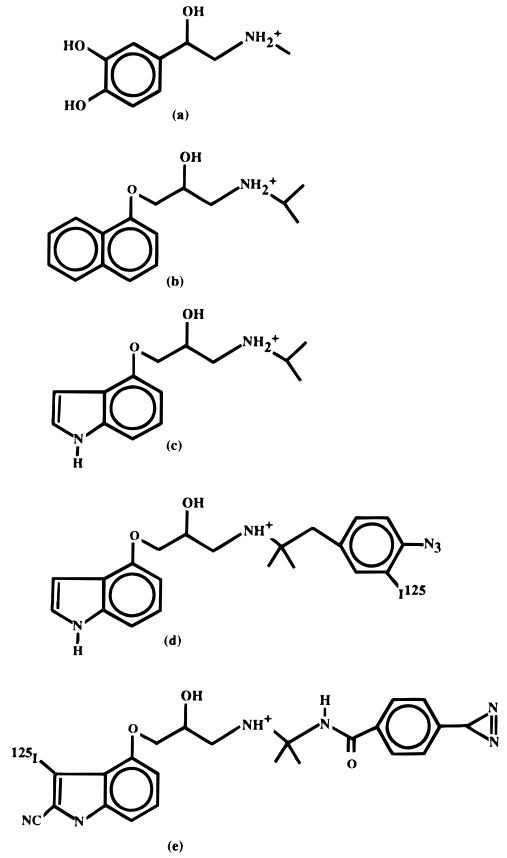

Suryanarayana has shown that this Asn is important for binding the ether oxygen of β-antagonists (see Chart 1) and plays a key role in the $\alpha-\beta$ switch. (Liu also found that better agreement between experiment and simple helical models could be obtained by rotating helix 7 slightly.[25]) Since the major current structural question probably relates to the secondary structure and orientation of helix 7 (see below), this is an important observation.

4. The transmembrane helix prediction algorithm also suggested that helix 4 should be shortened by three residues at the intracellular end and by two residues at the extracellular end. The new intracellular solvent/bilayer boundary is in good agreement with the site-directed spin-labeling studies of Farahbakhsh[22] (see Table 1).

5. Helices 1 and 2 were twisted from the previous model so that the side chain of Asn^{51} on helix 1 could interact with the side chain of Asp^{79} on helix 2; both of these residues are conserved. The work of Zhou et al. suggests that Asp^{79} makes an alternative contact with Asn^{322} on helix 7. This alternative contact is apparently in conflict with the observations of Suryanarayana,[24] and so in our composite 3_{10} model introduced below, Asp^{79} interacts with both Asn^{51} and Asn^{322}.

The information in Table 2, based on the multiple sequence alignment involving rhodopsin and the rat[26] β_1-, β_2-, and β_3-receptors, was used as a check on the receptor model, since all of these residues should probably face inward as they do in rhodopsin.[19] Indeed, these constraints were satisfied. In addition to the information based on rhodopsin given in Table 2, the β_2-adrenergic-specific mutation data in Table 3 were used to examine the model, and indeed the new model is consistent with all of the data in that all the transmembrane residues point inward. However, if the data of Zhou et al. and Sealfon et al.[27] on the possible interaction between Asn^{87} and Asp^{318} in the gonadotropin-releasing hormone receptor and similarly between Asp^{120} and Asn^{376} in the $5HT_{2A}$ receptor

Table 2. Residues Pointing Inward in Rhodopsin and the Corresponding Residues in the β_2-Adrenergic Receptor

helix	rhodopsin	β_2-AR	ref
1	Gly^{51}	Ile	91
	Thr^{58}	Val	91
	Asn^{55}	Asn	91
2	Gly^{90}	Val	92
	Asp^{79}	Asp	18
2	Glu^{113}	Trp	92
	Phe^{115}	Ser	93
	Ala^{117}	Asp	93
	Glu^{122}	Val	94
	Leu^{125}	Ile	91
	Trp^{126}	Glu	93
	Ser^{127}	Thr	93
4	Ala^{164}	Ser	95
5	Phe^{208}	Ser	96
	His^{211}	Ser	96
6	Phe^{261}	Phe	93
	Trp^{265}	Trp	93
	Tyr^{268}	Phe	97
	Ala^{269}	Phe	95
7	Ala^{292}	Asn	98
	Lys^{296}	Tyr	18

(Asp^{79} and Asn^{322} in β_2-AR) are taken into account, it is almost impossible for all of the functionally important residues to face inward, and indeed we will later argue that at least one of the functionally important residues should face the lipid. Because of this apparent conflict between the data of Suryanarayana and Zhou, two additional models with alternative orientations of helix 7 were built. The initial model, the one referred to unless otherwise stated, corresponds to the "312 model", the alternative model, i.e., the "322 model" ,satisfies the data of Zhou and Sealfon, while the composite model, which satisfies all of the data, will be referred to as the 3_{10} model.

The structure manipulation was carried out using the WHATIF molecular graphics program.[28] The final apo receptor models were refined by subjecting them to 10 steps of steepest descent and 9990 steps of conjugate gradient energy minimization followed by 1 ps of dynamics at 10 K, 5 ps of heating from 10 to 100 K, 20 ps of heating from 100 to 298 K followed by 40 ps of molecular dynamics at 298 K. The simulations employed the AMBER all atom force field,[29] as implemented in the AMBER 4.1 suite of programs.[30] The additional parameters required for the ligands were derived by analogy to existing parameters; the semiempirical AM1[31] potential derived charges were calculated using the *rattler* in-house software[32] since this gives charges consistent with those in the AMBER force field.[33] A distance-dependent dielectric constant was used, as described elsewhere.[14] A time step of 0.0005 ps and a nonbonded cutoff of 10 Å were used for the molecular dynamics simulations.

Docking. Using the 312 model, the ligands shown in Chart 1 were interactively docked across the A domain comprising of helices 1−5 using the conserved aspartate on helix 3 (Asp^{113}) as a guide to the initial placement of the amino group. The hydrophobic portion of the ligands was then aligned into one of the two hydrophobic pockets identified using GRID[34] with a CH_3 probe. The first pocket is formed by Met^{40}, Val^{44}, Ile^{47}, and Val^{48} on helix 1, Met^{82}, Gly^{83}, Val^{86}, and Phe^{89} on helix 2, and Val^{117} on helix 3. The second pocket is formed by Val^{114}, Ile^{154}, and Phe^{208} on helices 3−5, respectively. These pockets are complemented by corresponding regions on helices 7 and 6, respectively. This placement was aided by the hydrogen bond donor−hydrophobic distance distribution constraints identified during recent GRID-based receptor mapping studies.[14] The B domain comprising of helices 6 and 7 as then translated away in the membrane plane by 5−7 Å. The system was subsequently subjected to the same minimization and molecular dynamics procedure outlined above to enable the B domain to reassociate and form the final receptor−ligand complex (see Scheme 1).

Dynamic Aspects of the Receptor Structure. In order to analyze the structural changes resulting from the simula-

Table 3. Mutations Affecting Activity of the β_2-Adrenergic Receptor[a]

residue	mutant residue	effect	position	ref
Leu^{64}	Lys	increased agonist binding	I1	99
Asp^{79}	Ala	increased agonist binding	H2	12
Asp^{79}	Asn	reduced agonist binding	H2	100
Asp^{113}	Glu	reduced agonist/antagonist binding	H3	12, 13
Asp^{130}	Asn	increased agonist binding	H3	101
Pro^{138}	Thr	CAMP decreased (G-protein coupling?)	I2	99
Ser^{204}	Ala	reduced agonist binding	H5	12
Ser^{207}	Ala	reduced agonist binding	H5	12
Glu^{268}	Gly	agonist binding increased	I3	99
Cys^{285}	Ser	no maximal stimulation	H6	101
Asn^{312}	Ala	no antagonist binding	H7	24
Asn^{312}	Thr	reduced antagonist/agonist binding	H7	24
Asn^{312}	Phe	no binding of antagonist/agonist	H7	24
Ser^{319}	Ala	low agonist binding	H7	24
Tyr^{380}	Ala	lower CAMP production	C-term	103

[a] These data were used to model the apo receptor since the majority of these residues should point inward from within the transmembrane portion of the receptor. The data were also used to check the results from the docking process. H denotes helix; I denotes intracellular loop.

tions in the presence of the ligand, the simulations were continued for 500 ps. The changes were analyzed by superimposing the resultant time-averaged structures onto the time-averaged structure of the apo protein. The time averaging involved dumping coordinates every 50 ps (after the initial 100 ps since the major changes were essentially complete within the first 40 ps); the structural averaging was carried out using WHATIF.

Results and Discussion

The β_2-Adrenergic Receptor Model. 1. Ligand Binding and Orientation of Helix 7. The 312 receptor model was constructed in the absence of ligand to conform with the available experimental site-directed information (Tables 2 and 3). Most of the site-directed mutagenesis information was used to ensure that the key residues listed in Table 3 pointed inward from within the transmembrane portion. In the absence of a crystal structure, it is difficult to assess the quality of the model. However, the agreement with all of the data in Table 3 on ligand binding is encouraging. In particular, it is encouraging to observe interactions between the antagonist and Asn^{312} on helix 7,[24] since many previous models did not accommodate this. (The interaction between the agonist and Asn^{312} is indirect, involving a hydrogen-bonded network.) The antagonist interaction with Asn^{312} would not have arisen if the homology had not been shifted by two turns as described in the Methods section. In addition, the 312 model may explain why epinephrine has a 10-fold higher affinity over norepinephrine for the β_2-adrenergic receptor,[1,2] whereas in the β_1-adrenergic receptor the affinities are reversed. In the β_2-receptor model, the additional *N*-methyl group of epinephrine interacts with Leu^{311} on helix 7. This explains the lower affinity of norepinephrine since it cannot form such a strong interaction with the hydrophobic leucine residue. However, in the β_1-receptor, Leu^{311} is replaced by phenylalanine and so the protonated amino group of norepinephrine can form a $\pi-$hydrogen bond with the aromatic π-electrons,[35] thus explaining the affinities of both ligands for these receptors. Elsewhere we have performed high-level energy calculations on the interaction between the agonist and residue 311 which support this hypothesis.[36] (Lybrand commented on suggestions that interactions with helix 4 may explain the β_1/β_2 specificity of epinephrine and norepinephrine,[37] but no molecular explanation was given.)

Thus, our 312 model is consistent with two primary pieces of information which assist in confirming the orientation of helix 7: (i) the importance of Asn^{312} in antagonist binding[24] and (ii) the role of Leu^{311} in explaining the β_1/β_2-subtype specificity[38] of epinephrine and norepinephrine. In addition, there is the possible role of Ser^{319} in agonist binding. In Lybrand's 1992 and 1996 (clockwise) models,[37,39] hydrogen bonding between Ser^{319} and the β-OH group of epinephrine is given as the origin of the known preference for the *R* isomer over the *S* isomer, and this in turn is presented as a justification for the clockwise model; the interaction is also seen in our (anticlockwise) model. There is experimental support for this interaction with Ser^{319} as mutation to alanine affects agonist binding but not antagonist binding.[13] However, the effect is rather weak, and the stereoselectivity could also be explained by other interactions such as with Asn^{294} on helix 6 which is just one turn above Phe^{290}, possibly mediated by bound water molecules. Further evidence that Asn^{312} should face inward comes from mutation studies on the corresponding residue in other receptors. Adham has shown that mutation to Asn of the residue corresponding to Asn^{312} in $5HT_1$ receptors greatly increases the affinity for β-adrenergic antagonists such as propranolol and pindolol.[40] (This would imply that the partial agonist pindolol also binds in the antagonist binding site, whereas in our study it binds to the agonist binding site.) Wess has shown that mutation to Phe of the corresponding Tyr^{529} in the muscarinic M_3 receptor ensures that the agonists acetylcholine and carbachol no longer bind with high affinity; reductions in binding affinity were also observed for the antagonist [^{3}H]NHS but not for trihexyphenidyl.[41,42] Similarly, mutation of Ala^{292} to Glu in rhodopsin results in anomalous G-protein activation. Consequently, all of these residues should probably face inwards, and as a result their orientation is shown schematically in Figure 1a; this orientation is consistent with the simple helical model of Liu.[25]

The alternative arrangement, Figure 1b, required to satisfy Zhou's possible interaction, forces certain key residues, notably Asn^{312}, to face the lipid; likewise, Leu^{311} and Ser^{319} would be forced to point away from the binding site.

The advocates of the clockwise model, notably Lybrand and Weinstein[6,39,43] do not have a problem form-

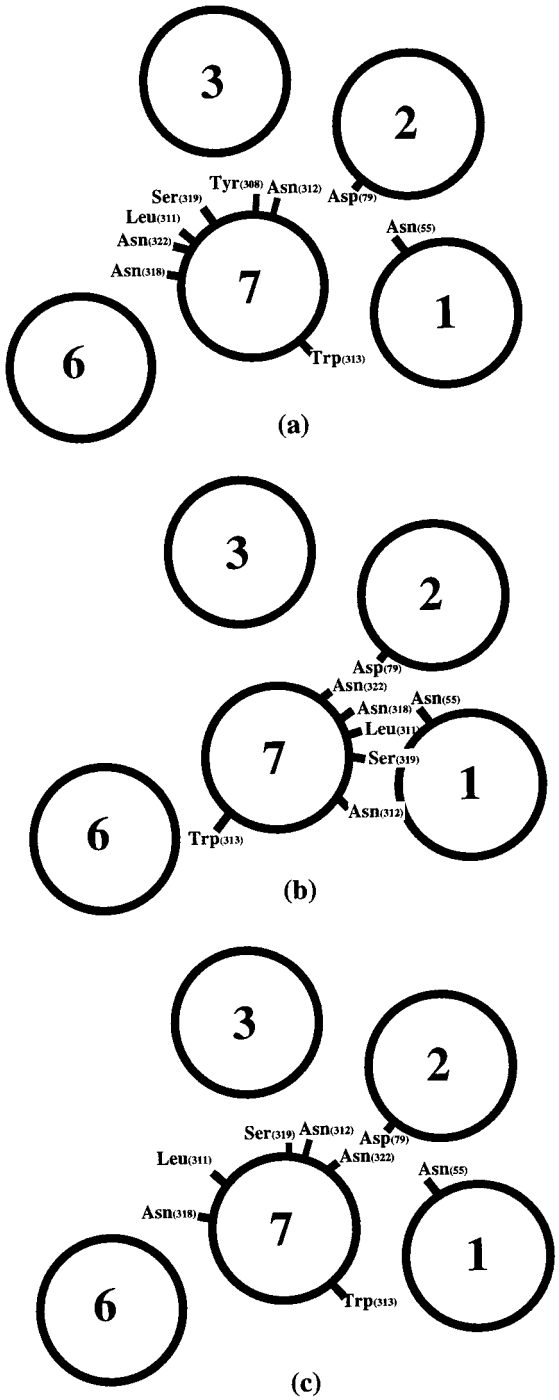

Figure 1. (a) Orientation of helix 7 in the current 312 model, (b) alternative orientation required to satisfy the data of Zhou and Sealfon, i.e., the 322 model, and (c) orientation of helix 7 in the composite 3_{10} model.

ing both the Asp^{79}−Asn^{322} interaction and drug interactions with Asn^{312}. However, it is not so straightforward to form both interactions using the more widely held counterclockwise (as viewed from the extracellular side) model. Thus, in order to analyze Zhou and Sealfon's helix 2−helix 7 interaction, it is essential to discuss whether the clockwise or counterclockwise model is correct. Since this has been analyzed many times in the literature, we will simply note that the gain of function mutational studies on chimeric receptors by both Liu et al.[25] and Mizobe et al.[44] provides strong support for the counterclockwise model; the latter study also provides evidence of a role for Leu^{311} in binding. Further strong evidence for the counterclockwise model is provided by the studies on the engineered zinc site in the neurokinin NK-1 receptor.[45] Thus, at this present time it does not appear possible to construct a clockwise model which is consistent with experiment. Even with a counterclockwise model, unless there is a distortion in helix 7, possibly caused by a short section of a 3_{10}-helix, which is certainly not impossible,[46] then it is impossible to satisfy all of these constraints *at the same time*. Thus, if we wish to retain a model consisting of essentially regular α-helices, we are forced to conclude that functionally important residues must face the lipid, at least for part of the mechanistic cycle. This situation is not necessarily problematic as will be discussed below. Here though we will simply note that there is a precedent for functionally important residues facing the lipid since Huang has observed that mutation of Tyr^{205} in the neurokinin NK-1 receptor results in loss of activity; Tyr^{205} is an external residue but was not identified as such.[47]

2. Helix 7 Secondary Structure. Recent work by Fu et al. suggests that it may be wrong to view helix 7 as a regular α-helix, or even as a regular α-helix containing a proline kink.[48] Using the substituted cysteine accessibility method, the water-accessible surface of the binding site on helix 7 of the dopamine D_2 receptor was identified, and it was concluded that the data were consistent with a kinked helix.[49] (Findlay also drew similar conclusions, but his kink was near the rhodopsin retinal attachment site.[50]) Certainly, there is a conserved proline at position 323, and this is likely to force some distortion at position 322 since the secondary structure assignment of Asn in Asn-Pro is not usually consistent with that of a *regular* α-helix.[48] Indeed, in our first model, which satisfies the interactions of Asn^{312} rather than those of Asn^{322}, the ϕ,ψ angles of Asn^{322} are −59°,−32° and are thus outside those of a regular α-helix and more akin to those of a 3_{10}-helix. Indeed, MacArthur has observed a number of incidences of 3_{10}-helices in X-Pro sequences,[48] though the X may also adopt ϕ,ψ angles which correspond to the β-region of the Ramachandran plot. Using interactive molecular modeling, we have investigated a range of ϕ,ψ angle combinations ranging from −150°,150° for the β-region through −71°,−18° for a 3_{10}-helix to −57°,−57° for a regular α-helix[51] to see which range of angles permit Asn^{322} to point toward helix 2, as required to satisfy the data of Zhou and Sealfon et al. Figure 2 shows that any combination between those for a 3_{10}-helix and those for the β-region is permissible in terms of orientation, but only the extreme values permit the Asn^{322} side chain to point well out toward helix 2 and indeed if Asn^{322} adopts a 3_{10}-helix conformation, the preceding two residues must also form part of a short section of a 3_{10}-helix if Asn^{322} is to point toward Asp^{79}. There is evidence to suggest that both possibilities for forming this interaction are possible.[46,48] However, if Asn^{322} adopts a β-conformation, then there will be a large distortion in helix 7 which is not observed in the rhodopsin cryomicroscopy studies, even though rhodopsin also contains the conserved NP motif. (Here we should note that the cryomicroscopy studies are not sufficiently sensitive to distinguish between an α-helix and a 3_{10}-helix; we should also note that 3_{10}-helices are usually observed in short sections of three to four residues.[51])

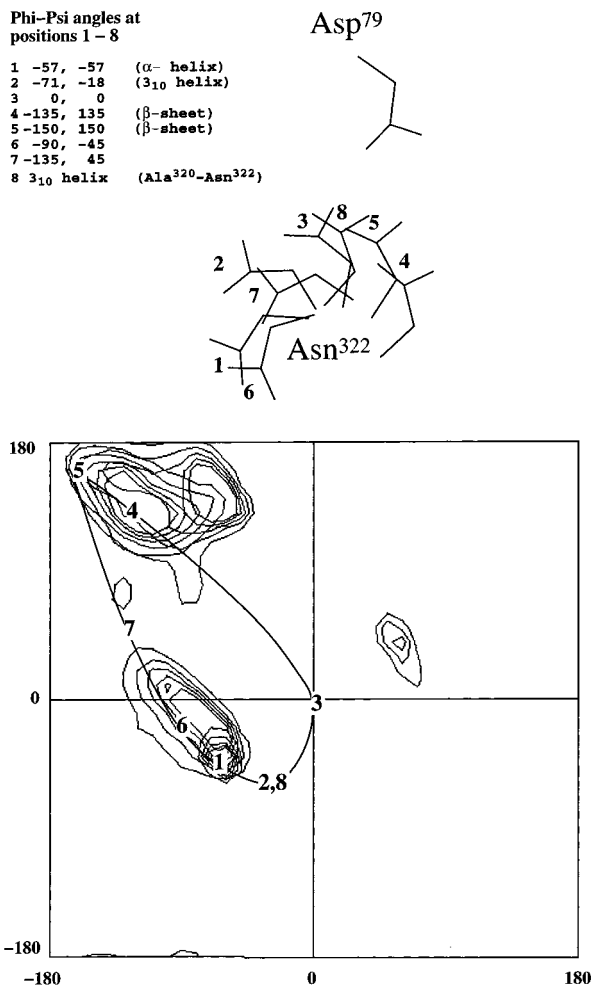

Figure 2. Schematic diagram showing the relative orientation of Asp^{79} on helix 2 and Asn^{322} on helix 7 as a function of the Φ,Ψ angles of Asn^{322}. A Ramachandran plot showing these angles is also given.

Fu et al. found that their data were readily explained by a major kink in the region of Asn^{322}. We have reexamined their data and found that the data are consistent with our 3_{10} model with the following provisos: Asn^{318} which has been identified as one of the accessible residues in the binding crevice is accessible, but it is near the boundary with helix 6. Similarly, although Trp^{313} is external in our model, as defined by the $C_\alpha-C_\beta$ vector, the side chain may point toward the helix 1−helix 7 interface. The photoaffinity-labeling studies of Wong[52] identified Trp^{313} as the major covalent product. This would suggest that Trp^{313} is clearly in the binding crevice, and support may be obtained from the site-directed mutagenesis studies of Wess.[53] However, it is not easy to place Leu^{311}, Asn^{312}, and Trp^{313} in the binding site, and so we interactively docked the photoaffinity reagents IABP and ICYP-da (Chart 1), using the information on pindolol binding. This yielded two important pieces of information. Firstly, it provided evidence that pindolol binds to the agonist binding site. Secondly, the putative carbene or nitrene from the IABP or ICYP-da points beyond Leu^{311} and Asn^{312} into the helix 1−helix 7 interface where it will readily interact with Trp^{313}. We conclude therefore that our positioning of Trp^{313} at the helix 1−helix 7 interface is consistent with the covalent binding studies and that the data of Fu et al. may be explained by a 3_{10}-helix. (A slight increase in the tilt angle of helix one would be sufficient to bring Trp^{313} much more into the binding site.)

At present there is probably insufficient data to distinguish between these two possibilities, a kink or a 3_{10}-helix, as one may conclude that both are energetically feasible.[46,48] Thus, the observation of a kinked helix 7 structure in dimethyl sulfoxide by NMR[54] does not imply that this structure will be obtained in a helix bundle within the lipid bilayer. Moreover, for the purposes of the current paper, the precise geometry below Ser^{319} is not significant as this region is not generally involved in ligand docking (though it does affect ligand affinity[55]). The XP motif also occurs in helices 2 and 4−6, but here X is either leucine or valine which is much less likely to be distorted;[48] there is no clear evidence for distortion at the XP in helix 5 from the substituted cysteine accessibility method (SCAM).[56] We conclude that by current standards a high-quality model structure will need to address the possible distortion around Asn^{322} arising from the conflict between the data of Suryanarayana and that of Zhou and Sealfon, and indeed our 3_{10} model satisfies these criteria.

3. Other Data on Helix Orientation. The data from studies of zinc binding to sites specifically engineered in the neurokinin NK-1, κ-opioid, or rhodopsin G-protein-coupled receptors[45,57−59] provide a further check on our structure since it provides distance constraints between different helices. Table 4 shows the range of possible His−His distances in our model obtained by mutating the homologous β_2-adrenergic residues to histidine. The zinc could bind to either N_δ or N_ϵ of each histidine side chain. The data show that our model is in full agreement with the studies based on zinc-binding sites at the top of helices 2, 3, 5, and 6.[45,57,58] The 1.6 Å discrepancy with the data of Sheikh et al.[59] arises because Val^{138} (Ala^{134} in β_2-AR) on the extension of helix 3 in our current model faces the lipid. (The data from Sheikh et al. on the orientation of helix 6 are in full agreement with our model in that the engineered histidine residues Lys^{248} and Arg^{252} (His^{269} and Lys^{273} in β_2-AR) which do not bind zinc, face the lipid.) The site-directed spin-labeling studies[21,22] give some indication of helix−helix contact points, and our orientation of helix 3 is in agreement with the data. The orientation of the binding crevice on helix 3 in our model is also in agreement with the substituted cysteine accessibility studies of Javitch[60] which place Val^{111}, Asp^{114}, Val^{115}, Cys^{118}, Ser^{121}, Ile^{122}, Asn^{124}, Leu^{125} and Ser^{129} in dopamine D2 (Thr^{110}, Asp^{113}, Val^{114}, Val^{117}, Ser^{120}, Ile^{121}, Thr^{123}, Leu^{124}, and Ala^{128}, respectively in β_2-AR) as internal residues. In addition, Siebert identified an interaction between Glu^{122} on helix 3 and His^{211} on helix 5 in rhodopsin (Thr^{118} and Ser^{207} in β_2-AR) using FT-IR spectroscopy and mutagenesis;[61] this interaction is also observed in our model. We therefore conclude that the discrepancy[62] with the data of Sheikh et al. arises either because the zinc-binding site on helix 3 is on a helix extension which may contain a flexible hinge region or since the resultant rhodopsin was unable to couple to transducin it may be that zinc binding to the engineered site has perturbed the structure, probably by rotating or tilting helix 3. It is probably true that the extracellular transmembrane portion of the receptor is better defined than the

Table 4. Apo β_2-Adrenergic Nitrogen−Nitrogen Distance Ranges Observed in Histidines Corresponding to Those Engineered To Bind Zinc in the Neurokinin NK-1, κ-Opioid, and Rhodopsin Receptors[a]

wild-type residues	β_2-residues	$C_\alpha-C_\alpha$ distances	N−N distances				
			$N_\delta-N_\delta$	$N_\epsilon-N_\epsilon$	$N_\delta-N_\epsilon$	$N_\epsilon-N_\delta$	ref
93−109	$His^{93}-Trp^{109}$	8.1	2.0−10.4	1.0−10.2	1.4−10.5	1.3−9.9	45
109−193	$Thr^{110}-Asn^{196}$	8.8	3.8−6.6	3.1−6.5	3.6−6.0	3.5−6.2	45
197−290	$Ala^{200}-Phe^{290}$	8.7	1.5−11.3	1.6−11.5	1.9−11.0	1.7−11.6	57
223−298	$Asn^{196}-Val^{297}$	8.4	1.2−8.3	1.0−8.1	0.9−8.4	1.3−8.6	58
227−298	$Ala^{200}-Val^{297}$	10.8	0.0−5.8	0.0−6.0	0.0−5.9	0.0−6.1	58
138−251	$Ala^{134}-Leu^{272}$	14.6	11.8−18.1	10.9−17.8	11.1−18.0	11.5−18.1	59

[a] The distances were obtained using intermolecular graphics to sample all the sterically accessible conformations of the histidines. For zinc binding, the N−N distance should be about 3.2 Å as, for example, observed in the carbonic anhydrase crystal structures or the $C_\alpha-C_\alpha$ distances should be no greater than about 13 Å as described in ref 62.

Table 5. Assessment of the Structure of the Current Model According to the Site-Directed Spin-Labeling Studies[22,21] [a]

helix	residue no.		mobile or immobile	contact in model
	rhodopsin	β_2-AR		
3	136	Y132	immobile	helix 6
3	137	V133	mobile	lipid
4	152	K149	mobile	lipid
4	153	A150	mobile	helices 5 and 6[b]
4	154	R151	mobile	lipid/helix 3
5	225	R221	mobile	lipid
5	226	V222	immobile	helix 4
5	227	F223	mobile	helix 6[b]
6	251	L272	immobile	helix 5
6	252	K273	mobile	lipid/water
6	253	T274	immobile	helix 7
6	255	G276	mobile	lipid/water

[a] The analysis considers residues in the transmembrane region but not in the helix extensions. [b] This residue is at the end of the helix and is fully exposed; we would therefore expect it to be mobile.

intracellular portion because more ligand binding data are available, but we do not believe this is the main problem here.

The site-directed spin-labeling studies[21,22] have confirmed that our bilayer/solvent boundary residues are in agreement with experiment, as shown in Table 1; they also enable us to identify immobile residues which suggests that the residues are involved in secondary interactions, for example, at the helix−helix boundaries. In Table 5 we have tabulated these data, and we can indeed associate the mobility of the nitroxide spin-label with our structure. Again, the comparison shows that our model is in good agreement with experiment. Even more interesting is the change in mobility upon photoactivation. The mobility of residue 227 in rhodopsin is intermediate between that of an exposed residue and that of a buried residue, but on activation it becomes much less mobile. In our simulation (see below) there is a rotation in helix 5 of about 20−30° which would move this residue into the helix 5−helix 6 interface, thus reducing its mobility and showing agreement between experiment and our activation mechanism even though intracellular loop 3 has a very different length in the two receptors. Finally, the hydropathy profiles[63] for rhodopsin and the β_2-adrenergic receptor are shown in Figure 3. Superimposed on this figure are the β-turn predictions[64] which may be indicative of flexibility in helical regions. There are clear indications in both the profile and the predictions that there may be subtle differences between the two structures, and so cross-receptor comparisons should be undertaken with care.

The orientation of helix 5 is well defined by the serine mutation studies, the site-directed spin-labeling studies, and the zinc binding studies. However, the substituted

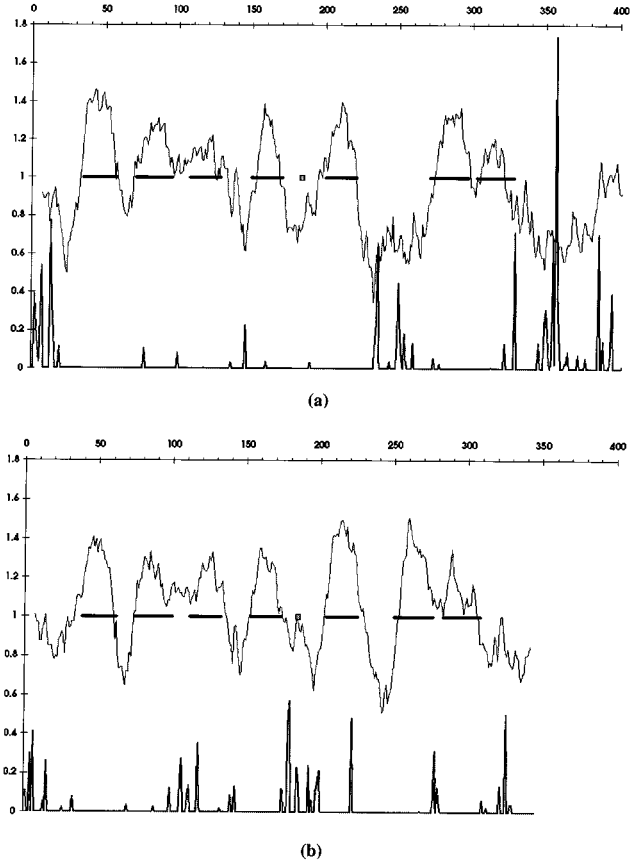

Figure 3. Hydropathy profile and β-turn predictions for (a) rhodopsin and (b) β_2-adrenergic receptor. Note that a turn is predicted at the cytoplasmic end of helix 3 in profile b but not in profile a.

cysteine accessibility method showed that the consecutive dopamine D2 residues Tyr^{192}, Ser^{193}, Ser^{194}, and Ile^{195} on helix 5 (equivalent to Ala^{202}, Ser^{203}, Ser^{204}, and Ile^{205} in β_2-AR) were all accessible to reagents which react with accessible cysteines[56] even though they are clearly on different faces of the helix. Two interpretations were given: the first is that helix 5 may unwind; the second is that helix 5 may rotate. In our model, helix 5 is part of the hinge region between the A and B domains, and as we observe rotation in helix 5 during simulations on the receptor−agonist complex, the latter explanation is probably more correct. However, interactive molecular graphics suggest that the cationic reagents MTSEA and MTSET and the anionic reagent MTSES[56] react with accessible cysteines primarily where there is a suitably placed counterion such as Asp^{80} on helix 2, Asp^{114} on helix 3, and His^{394} on helix 6 (Asp^{79}, Asp^{113}, and Asn^{295} in β_2-AR, respectively). (The dependency of the results on charge explains several

anomalies in the results such as why the primary Ser[197] which binds the para catechol OH group was not affected by MTSES.) Thus, there is a distinct possibility that these SCAM studies are introducing perturbations, such as helix rotations, into the structure in order to form an appropriate salt bridge; it is possible too that the "kink" observed in helix 7 has been exaggerated for a similar reason. Thus, the SCAM results on all the helices, like the photoaffinity-labeling studies,[52] should be interpreted with reference to a suitable model which may indicate whether such perturbations are likely. When allowance is made for these possible artifacts, our model is in agreement with the substituted cysteine accessibility method.

4. Comparison with Other β_2-Adrenergic Receptor Models. Further evidence for the quality of our structure comes by comparing the structure to other quality models where coordinates have been made available, notably the Donnelly and Bywater models.[65,66]

The Donnelly β_2-adrenergic receptor model[65] was also based on rhodopsin. Helices 1 and 2 are slightly more tilted in the Donnelly model; the helices are also consistently longer, and this could cause problems with loop modeling. However, this is probably not a major problem since the helix ends are not precisely defined and because Donnelly does not distinguish between the bilayer solvent boundary and the helix ends. Helix 3 is less buried by helix 4 in the Donnelly model, and helices 4 and 7 have a 7−8 Å translation in the membrane plane. Finally, Donnelly notes that helix 7 needs remodeling to accommodate Asn[312] in the helix bundle.

In the Bywater β_2-adrenergic receptor models,[66] the rotational positioning of all helices is generally similar to that in both our model and the Donnelly model. The first Bywater model, presented for historical reasons, is based on bacteriorhodopsin, and consequently there are large displacements in the intracellular regions of helices 4−6 due to the differences in the tilt angles. Helix 7 is shifted 5−6 Å toward the intracellular end of the receptor. The second Bywater model is based on rhodopsin and differs from the first largely in the way the helices are packed together. The transmembrane segments used to build these models, the Hibert model[67] and the Lybrand 1996 model[39] (for which coordinates have not been deposited), are shown in Table 1. The Lybrand structure is a clockwise model, and so the structure is not discussed for the reasons given above.

It is clear from this comparison that the agreement is generally very satisfying in terms of helix rotation and placement within the membrane plane but less satisfying in terms of helix positioning along the perpendicular to the plane. However, a relatively large 5 Å displacement of, say, helix 5 may only have a small effect (≤1 Å) on the distance between the serines on helix 5 and the conserved aspartate on helix 3. Consequently, the 312 model (and the 3_{10} model) is satisfactory for testing the new approach to docking, and the coordinates have been deposited at EMBL[68] and as Supporting Information. The structural differences between the various β_2-adrenergic models in the literature probably arise because the underlying potential energy surface is very flat, conferring the receptors with very dynamic structures. Indeed, in the following section we propose that domain movement in the membrane plane is as important as movement perpendicular to the plane.

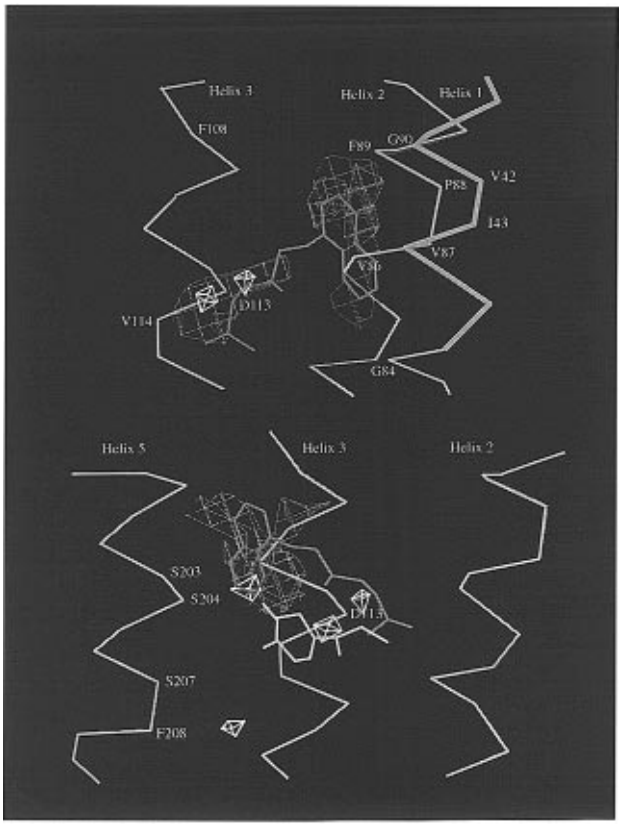

Figure 4. Schematic diagram showing the two hydrophobic pockets on the A domain. (a, Top) Large contoured region associated with the antagonist-binding site, as identified using a CH_3 GRID probe. The energy contours for a GRID NH_4+ probe which occur near Asp[113] are also shown. (b, Bottom) Large contoured hydrophobic pocket associated with the agonist-binding site. Again, the contours for a GRID NH_4+ probe which occur near Asp[113] are shown, as are the contours arising from a GRID OH probe; these two small OH contours are situated near the two serines on helix 5; the contour near Ser[207] is of lower energy as it is augmented by interactions with the backbone carbonyl of Ser[207].

Docking. In our initial studies,[14] we encountered difficulty in docking ligands because of the steric restrictions arising from interactions with the aromatic residues on helix 6 (Trp[286] and Phe[290]). The problem was magnified because of the restricted space within the apo receptor model compared to the ligand-bound forms, as shown by interactive molecular graphics[28] and GRID maps[34] (results not shown). Thus, the computational advantage of pulling out the B domain is that it creates space to permit greater phase space sampling during the ensuing molecular dynamics. Clearly, despite the advantages of this approach, the multiple minima problem remains, and so the increased phase space sampling permitted by this new method is limited. Consequently, as in the model building as much additional information as possible was used to guide the docking process. Here we have used both calculated GRID potentials and site-directed mutagenesis information. The two hydrophobic pockets on the A domain, identified using GRID with a CH_3 probe, are shown schematically in Figure 4. The first pocket (Figure 4a), complemented by Asn[312] and Tyr[308] on helix 7, contributes to the antagonist-binding site; the second pocket (complemented by Phe[282], Trp[286], and Phe[290] on helix

6) (Figure 4b) contributes to the agonist-binding site. Association of the first hydrophobic pocket with the antagonist-binding site comes largely through the site-directed mutagenesis studies of Suryanarayana[24] who showed that Asn^{312} played an important part in binding β-selective antagonists which had an ether oxygen. The observation that mutation of the homologous residue in related receptors only affects some antagonist[42] binding may be an indication that not all antagonists bind to the antagonist-binding site, and as mutation of residues in the agonist-binding site may affect antagonist binding,[53,69] it is possible that some antagonists bind in the agonist-binding site. Association of the second hydrophobic pocket with the agonist-binding site comes through the work of Strader[13] in identifying the key role in binding played by Ser^{204} and Ser^{207}. These studies are complemented by the work of Hwa who showed a key role for Ser^{204} on helix 5 and Met^{314} on helix 6 in agonist binding but not antagonist binding, providing further evidence that the antagonist binds at the other end of the receptor, i.e., toward helices 2 and 7 rather than 5 and 6. The key role played by helix 7 in antagonist binding has also been shown by the chimeric receptor studies of Kobilka.[70] Thus, the key information which arose from the GRID maps and the experiments was that there were only two key ligand starting orientations to be considered, as illustrated in Figure 4, namely, that the hydrophobic part of the ligand should generally point toward one of these two hydrophobic pockets. For the catecholamines, this is almost equivalent to starting with the catechol hydroxyl groups pointing toward Ser^{204} and Ser^{207} on helix 5. Thus, improved phase space sampling was observed in the sense that any initial orientation started from within these two regions gave essentially equivalent results. Here, it appears that only one simulation was required, but in other cases there may be benefits from multiple simulations. Using this method it is perfectly possible to dock an antagonist into the agonist-binding site, and it will not move into the other site. Indeed, the evidence presented above suggests that this should not necessarily be seen as undesirable. Indeed, this is how some authors model antagonist binding.[39]

Another advantage of this domain-based docking process is that the freedom of the B domain allows the vertical alignment of the domains to be partially optimized in the presence of the ligand. Table 6 compares the ligand−receptor interactions observed in our current model with those reported in other models. Since coordinates were not deposited for all of the other models, the comparison may not be complete. However, it would appear that the new model is consistent with the site-directed mutagenesis information. In view of the experimental evidence on the key role played by helix 7 in binding, particularly to antagonists, it is very interesting to observe interactions between the antagonist and Leu^{311} and Asn^{312} and also between the agonist and Leu^{311} and Gly^{315} (and Ser^{319}). These interactions are particularly noteworthy as neither the model nor the docking procedure was modified to generate them. In a related article we have presented a correlated mutation analysis of subtype specificity among various receptor families, including the β-adrenergic receptors.[38] We observed that while the agonist tends to bind to the conserved residues, such as the serines on helix 5, the antagonist tends to bind to the "correlated" residues,[71] and so the relevant correlated residues are shown in Table 4 for completeness.

Hibert reported an interaction between the β-OH group of the agonist with Ser^{165}. This would appear to be supported by the site-directed mutagenesis information on Thr^{164} as mutation to Ile markedly decreases agonist binding. However, this mutation also affects antagonist binding even though the evidence strongly suggests that antagonists bind elsewhere. Since both of these residues are involved in a hydrogen-bonded network which includes Glu^{122} on helix 3, it is likely that the effects due to the Thr^{164} mutation result from global rather than local deformations, as suggested by the authors. Consequently there is not necessarily any support from site-directed mutagenesis for the interaction of ligands with Ser^{165}, and indeed we did not observe such an interaction.

All of the models in Table 6 show "perpendicular" interactions with Trp^{286} and Phe^{290}. The agonist is pulled away from the initial hydrophobic pocket on the A domain by the attraction to the serines on helix 5 and as a result forms these new hydrophobic interactions. (The antagonist generally does not display such movement and so remains in the antagonist hydrophobic pocket.) In addition to site-directed mutagenesis support for these interactions in the β_2-adrenergic receptor, we note that these residues are widely conserved, and additional evidence for their importance in ligand binding comes from mutational analyses on the muscarinic M_3 receptor[53,69] and the $5HT_2$ receptor;[72] the neighboring tyrosine (equivalent to Phe^{289}) is also critically involved in binding muscarinic and serotonin ligands in the M_3 and $5HT_2$ receptors, respectively[41,72] but in our model Phe^{289} cannot make direct contact with the agonist because of steric restrictions.

Since hydration is not treated explicitly in these receptor simulations, it is essential to ensure that this is not the origin of any artifacts. The most likely artifact is the observation of binding to sites which would normally bind water molecules. To identify sites where hydroxyl binding should probably not occur, we have carried out GRID calculations using both a hydroxy probe and a water probe and displayed the difference between the two as a series of contour maps. The only relevant sites where the water had a clear preference were the aspartates, including Asp^{113} on helix 3, and the backbone carbonyl group on Ser^{207}. In our model there was a tendency in very long simulations for helix 5 to rotate so that the catechol could bind to the hydroxyl and carbonyl groups of Ser^{207} (rather than to the hydroxyl groups of Ser^{204} and Ser^{207}). Similar results have been observed elsewhere.[73] The GRID maps strongly suggest that this is an artifact and indeed one that can be eliminated by extending helices 5 and 6 to include a couple of turns of the N- and C-terminal ends of intracellular loop 3 since the additional helix−helix attraction counteracts the torque. (Since Ser^{204} is not required for binding in the α_{1b}- and α_{2A}-receptors, this carbonyl interaction may be genuine, but the GRID results and the site-directed mutagenesis studies[13] suggest that it is not.) The rational for extending helices 5 and 6 beyond the bilayer/solvent boundary comes from the helix prediction studies,[74] insertion mutagenesis studies on helix 6,[75] and site-directed spin-labeling

Table 6. Residues Involved in Agonist/Antagonist Interactions and Site-Directed Mutagenesis Studies[a]

			current		alternate		Lybrand 1992[39]	Lybrand[39]		Trumppkallmeyer[67]	Donelly[65]
residue no.	mutated	correlated	Ag	Ant	Ag	Ant	Ag	Ag	Ant	Ag	Ag
							Helix 1				
Ile[38]		*		*		*					
Met[40]		*		*		*		*	*		
Val[44]				*		*			*		
Ile[47]		*		*		*					
Val[48]				*		*					
Val[52]		*		*		*					
							Helix 2				
Met[82]				*		*					
Gly[83]		*		*		*					
Val[86]				*		*			*		
Phe[89]		*		*		*		*	*		
Gly[90]		*		*							
Ser[92]									*		
His[93]									*		
							Helix 3				
Trp[109]										*	
Thr[110]											
Asp[113]	*		*	*	*	*	*	*	*	*	*
Val[114]			*		*						
Cys[116]									*		
Val[117]			*		*			*	*		
Thr[118]			*		*						
Ser[120]									*		
Ile[121]			*		*						
							Helix 4				
Thr[164]	*									*	
							Helix 5				
Ser[204]	*		*		*		*	*		*	*
Ser[207]	*		*		*		*	*	*	*	*
Phe[208]										*	
							Helix 6				
Trp[286]	*		*		*		*	*	*		
Phe[289]	*									*	*
Phe[290]	*		*		*		*	*	*		*
Asn[293]											*
							Helix 7				
Tyr[308]				*						*	
Leu[310]					*	*					
Leu[311]		*	*	*							
Asn[312]	*	*		*					*		
Trp[313]											*
Gly[315]			*					*	*		
Tyr[316]	*								*	*	
Val[317]					*	*					
Asn[318]									*		
Ser[319]	*		*					*	*		*
Asn[322]									*		

[a] In our model, an interaction is loosely defined as two atoms roughly in van der Waals contact; other authors may have used a different measure, and this is probably the origin of most of the discrepancies reported below. Residues identified by a correlated mutation analysis are also shown. Coordinates were available for the Lybrand[39] and Donnelly[65] models.

studies.[21] Most of the other interactions listed in Table 6 were observed in the other studies and so will not be discussed further.

Figure 5a shows a stereoview of the interactions between norepinephrine and the receptor; Figure 5b shows a stereoview of the interactions between propranolol and the receptor, and Figure 5c shows a stereoview of the interactions between pindolol and the receptor. The docking was essentially complete within the first 40 ps, but the simulations were continued for at least 250 ps to confirm that the ensuing structural changes led to stable structures. It is possible that this new approach to docking may be successful because it mimics the natural process. Kobilka and Maggio have shown that coexpression of the individual A and B domains can lead to active receptors,[4] and so the ability of helices 6 and 7 to reassociate with the complementary domain is well documented; similar effects are seen with the "tryptic core" of the receptor.[76] More noteworthy still is Maggio's observation on chimeric receptors.[5] He observed that chimeric α_2-adrenergic (gray helices, Scheme 2)−muscarinic M_3 (black helices, Scheme 2) receptors are inactive, as are the alternative muscarinic M_3−α_2-adrenergic chimeras. However, active receptors are found when the two chimeras are mixed. Elsewhere we have proposed that the most likely explanation of this is that the active receptors are domain-swapped dimers[77] formed by the mechanism shown in Scheme 2. The role of domain swapping in dimer formation in general is discussed elsewhere,[78] and here we simply note an interesting observation of Tegoni et al. who

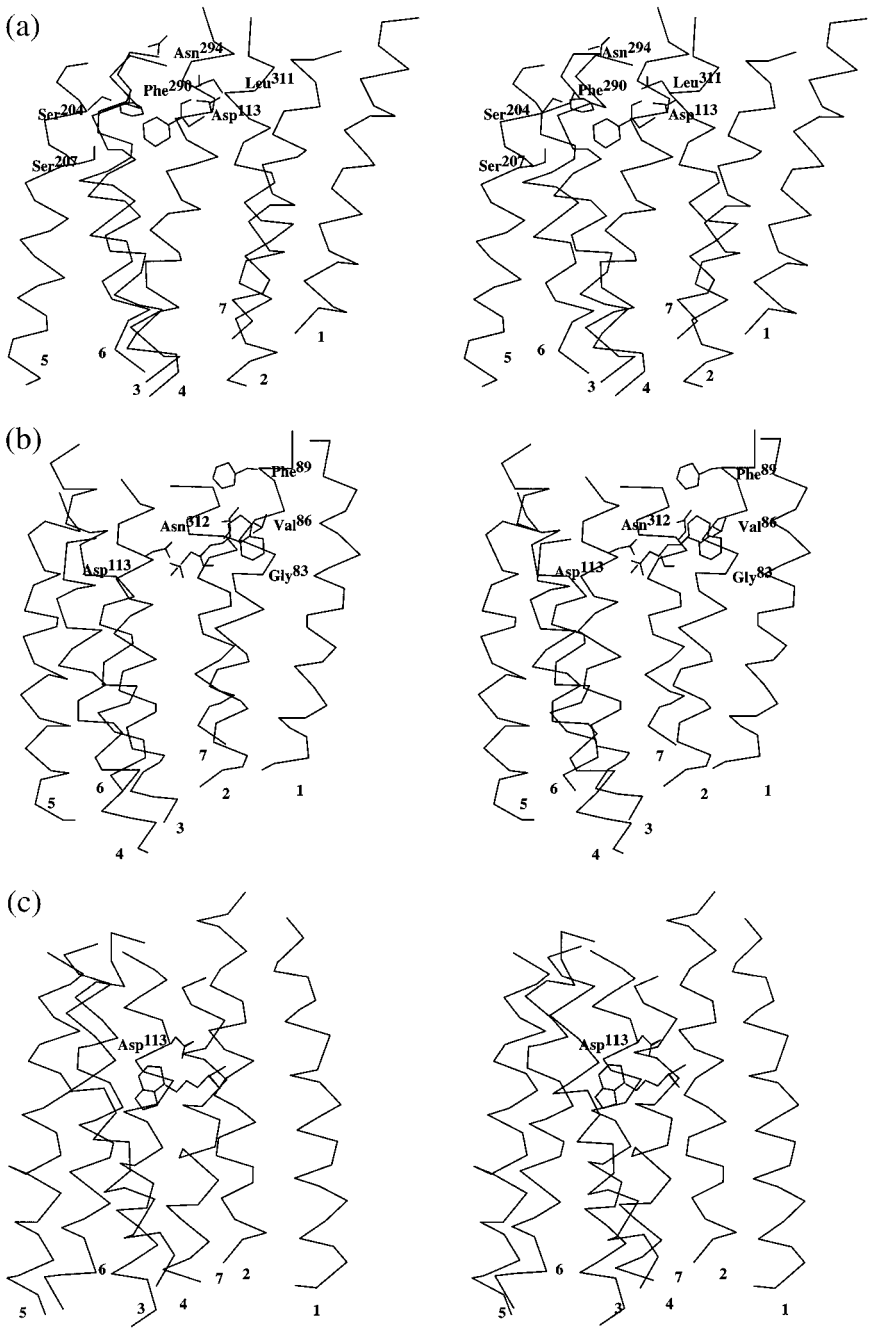

Figure 5. Stereoview of the interactions between the receptor and (a) norepinephrine, (b) propranolol, and (c) pindolol.

Scheme 2. Proposed Domain-Swapping Rearrangement[a]

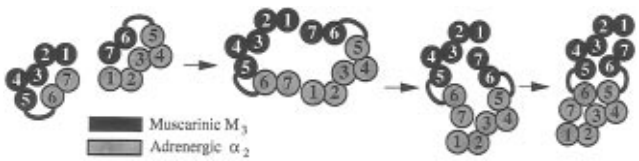

[a] For clarity, the dimerization is illustrated using chimeric adrenergic (gray)−muscarinic (black) receptors. The rearrangement may proceed without disrupting the domains containing either helices 1−5 or helices 6 and 7.

observed that the binding site in an odorant binding protein was formed by a domain swapping dimerization.[79]

It is possible that pulling the B domain out during the docking process mimics this rearrangement. Indeed, some domain opening may even be essential for ligand binding as it creates space for the ligand to pass through the canopy and enter the helix bundle. The hinge loop between the domains (intracellular loop 3) is frequently the longest loop in the receptor, and this will certainly permit large relative movement between the two domains. Indeed, Maggio has shown that activity is suppressed if this loop is shortened.[80] The recent publication of Hebert et al.,[81] which includes some interesting site-directed mutagenesis results, has shown the importance of helix 6 in dimer formation, providing further experimental justification for this domain-based docking methodology. The analogous work of Ng in showing that helix 7 can also inhibit dimer formation is significant,[82] but here the peptide is more likely to inhibit the formation of the 1,7-intermediate on the domain-swapping pathway than to block the dimer interface.

A cursory glance at the work of Schöneberg et al. on

the muscarinic M_3 receptor[83] and of Ridge et al. on rhodopsin[84] would suggest that G-protein-coupled receptors are composed of not two but multiple folding domains, and regarding binding this appears to be true—see Table 1 of ref 85—as coexpression of receptor fragments split in the intracellular or extracellular regions after helix 2, 3, 4, or 5 generally allows ligand binding. However, receptors are only able to couple to the G-protein if they are split in extracellular loop 3 and intracellular loop 3. Only in the latter case did Schöneberg observe wild-type activity. In rhodopsin, the receptors cut in extracellular loop 3 displayed activity more closely resembling that of the wild type, but here intracellular loop 3 is much shorter and may have been cut in a region essential for G-protein coupling. Moreover, Monnot has shown that coexpression of angiotensin-II receptors, with loss of function mutations, on either helix 3 or helix 5 can lead to functional rescue, as measured by ligand binding but not as measured by G-protein coupling.[86] This limited functional rescue can be explained by domain swapping where the extracellular loop between helices 4 and 5 is the hinge loop, enabling the loss of function mutations to be swapped out.[74] However, here the lack of G-protein coupling would tend to rule out helices 1−4 and helices 5−7 as functional domains. Thus, on balance, the experimental evidence currently suggests that the A and B domains are the primary folding domains in G-protein-coupled receptors.

Structural Changes. The major conformational changes observed during the simulations fall across the boundary between the A and B domains and generally occur in the intracellular half of helices 5 and 6. This is in agreement with experimental information on the key role played by intracellular loop 3 in the activation of G-protein-coupled receptors.[2] Figure 6a,b show a superposition of helices for the apo and antagonist-bound receptor. The antagonist structure is more open at the extracellular side than the apo structure, but the intracellular side of the receptor is virtually identical, with only minor structural changes.

The agonist-induced structural changes are shown in Figure 6c,d. Large movements in helices 5 and 6 are observed at the intracellular side of the receptor, and these may be sufficient to induce a conformational change in the intracellular loop which in turn activates the G-protein. Alternatively, change in the helix tilt angle may enhance the formation of the 5,6-domain-swapped dimer (Scheme 2) through a more optimal helix packing at the interface between two receptors containing one molecule of agonist.[77] In the apo receptor, helices 5 and 6 are essentially perpendicular to the membrane, but in the agonist−receptor complex there is a change in the tilt angle of helices 5 and 6 of approximately 20°. The changes in the monomers are essentially the same as those in the dimer,[77] and so the origin of the ligand-induced stabilization of receptor dimers is apparent. In addition to these changes in tilt angle, there is a relatively large vertical movement in helix 5.

The site-directed spin-labeling studies on rhodopsin are generally in agreement with these results in that much larger changes are observed in helices 5 and 6 than in helices 3 and 4. Altenbach et al. did not see such large changes in helix 5 as in helix 6, but in

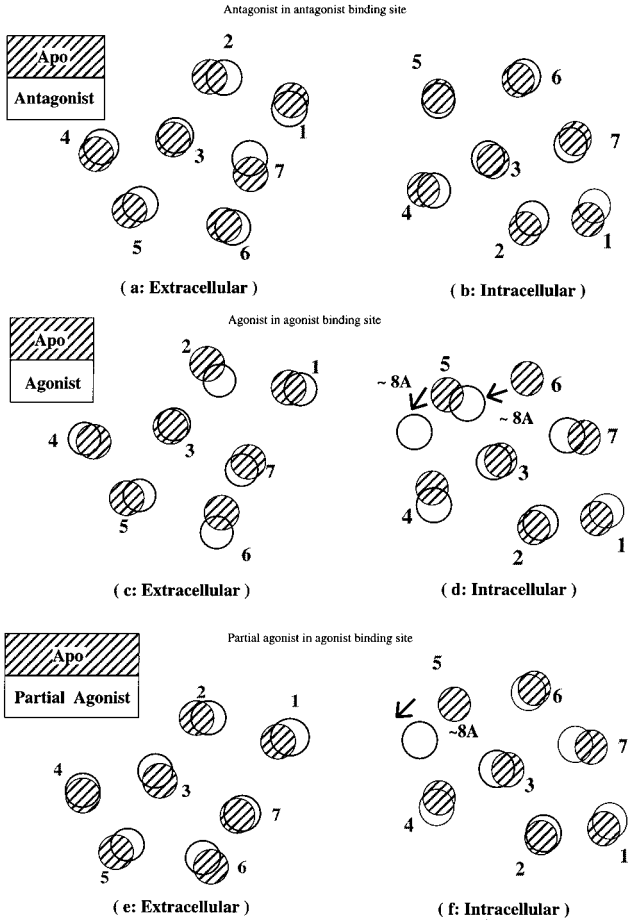

Figure 6. Superposition of the ligand-bound receptors onto the apo receptor: (a, b) superposition of the antagonist-bound receptor onto the apo receptor (with the antagonist bound to the antagonist-binding site), (c, d) superposition of the agonist-bound receptor onto the apo receptor, and (e, f) superposition of the receptor containing the partial agonist onto the apo receptor. As in Figure 7, the circles represent the positions of the ends of the helices as viewed from the extracellular or intracellular side of the membrane. Average structures from the molecular dynamics simulations were used, as described in the Methods section.

rhodopsin, intracellular loop 3 is very short (13 residues) while in the β_2-adrenergic receptor it is 60 residues. Support for large changes in helix 6 comes from the SCAM studies of Javitch et al.[10] and the fluoresence studies of Gether et al. on agonist-induced and constitutive activation;[7,9] these results could be explained by a rotation in helix 6, as observed in our studies, but in the absence of more precise molecular information it is difficult to quantify the agreement. In addition, there may be no need for rhodopsin to domain swap since its ligand, whether this is viewed as retinol or as a photon, does not have any barriers to binding (see above). Thus, rhodopsin may be quite different to other G-protein-coupled receptors.

The structural changes induced by the partial agonist pindolol are shown in Figure 6e,f. Although the molecular basis of partial agonism is not understood, it is interesting that here the structural changes induced by the partial agonist at the intracellular side (where interaction with the G-protein occurs) are midway between those for the agonist and those for the antagonist in that helix 5 shows a large movement similar to that in Figure 6c,d but helix 6 does not. There are also changes on the extracellular side, but these may not

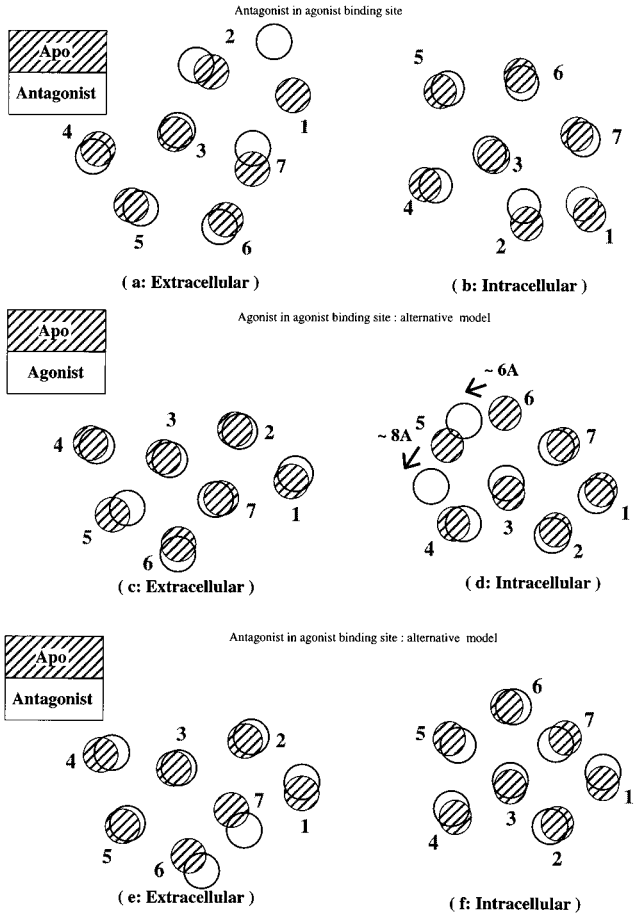

Figure 7. Superposition of the alternative ligand-bound receptors onto the apo receptor: (a, b) superposition of the antagonist-bound receptor onto the apo receptor (here the antagonist was docked into the agonist-binding site), (c, d) superposition of the receptor containing the agonist onto the alternative apo receptor, and (e, f) superposition of the antagonist-bound receptor onto the apo receptor in the alternative model structure (with the antagonist bound to the antagonist-binding site).

affect G-protein coupling. The docking strategy presented here may be useful in further study of this effect.

Jarv has proposed that an antagonist binding to an agonist-binding site will function as an agonist. Jarv's work is significant as he used a mathematical model involving two binding sites on one receptor to provide an explanation of bell-shaped dose−response curves.[87] In order to test his ideas, we have simulated the structural changes in the receptor in response to an antagonist binding to the agonist-binding site. The results are essentially the same as for an antagonist binding to the antagonist-binding site (see Figure 7a,b). Since bell-shaped dose−response curves are generally characteristic of dimerization,[88] we propose that the two binding sites required by the mathematics are the two agonist-binding sites in the 5,6-domain-swapped dimer. Our simulation results in Figures 6 and 7 provide a molecular justification for such a model as they suggest that a second agonist binding to the 5,6-domain-swapped dimer would cause large changes in the tilt angles of helices 5 and 6 resulting in the helix packing moving away from the optimal packing angle of about 20°. This would destabilize the dimer and result in reduced activity.

In order to relate these changes to experimental observations, we have investigated the electronic influence of Lys^{267} (on the intracellular side of helix 6, close to intracellular loop 3) and Arg^{83}, which is part of the conserved DRY motif on helix 3, since mutating either of these residues to an uncharged residue results in a loss of activity.[89] The residues were mutated to a neutral, deprotonated form. The resulting structure (not shown) is comparable to that obtained with pindolol and is therefore consistent with reduced activity.

Finally, because there is some doubt about the orientation of helix 7, we have repeated the simulations for the agonist and the antagonist (in the antagonist−binding site) using the alternative 322 model. The results for the agonist−receptor complex shown in Figure 7c,d are clear, in that they are essentially the same as those shown in Figures 6c,d. Likewise the antagonist results (Figure 7e,f) are essentially the same as those shown in Figure 6a,b. Thus, these changes appear to be an overall property of the receptor rather than an artifact arising from small scale uncertainties.

Finally, the helix 1−helix 7 interaction is probably the weakest in the whole receptor as it is the only one which involves parallel helix dipoles, and this could facilitate the initial opening of the receptor at the start of the domain-swapping pathway.

The domain-swapping mechanism shown in Scheme 2 may offer an alternative explanation for the apparent conflict between the data of Zhou et al. and Sealfon et al. on the one hand and that of Suryanarayana on the other. One possible explanation is that the interaction of Zhou and Sealfon is required to assist in rotation of helix 7 as a first step along the domain-swapping pathway. Indeed, this is not inconsistent with their report as Sealfon suggests that the conserved aspartate on helix 2 is involved in allosteric modulation—see also ref 90—since mutation of Asp^{79} may not always affect G-protein coupling. Taken together, the structural observations in Figures 6 and 7 may shed light on the activation mechanism since they are in line with a fairly consistent picture which is beginning to emerge from this and related studies.[6]

Conclusions

A new model of the β_2-adrenergic receptor has been presented which is consistent with both the known site-directed mutagenesis information on the β_2-adrenergic receptor and the corresponding experimental constraints derived from studies on the homologous rhodopsin; the model is also consistent with other biophysical data including the substituted cysteine accessibility studies, the site-directed spin-labeling studies, and the zinc binding studies. The model was built in the absence of ligand and used to test a novel approach to ligand docking. The approach involves partially docking the ligand onto the A domain containing helices 1−5 and allowing the B domain containing helices 6 and 7 to reassociate during the course of a molecular dynamics simulation (Scheme 1). The resulting receptor−ligand complexes were consistent with the known ligand binding data, including the site-directed mutagenesis information on Asn^{312} on helix 7. GRID difference maps were used to check that there were no artifacts among the observed receptor−ligand contacts arising from the treatment of hydration. The success of the new approach to docking arises (a) because it enables the ligand to sample phase space more freely and (b) because it

mimics the domain dynamics of the natural process. The ligand-induced structural changes give further support to the model and docking strategy. Firstly, they show that the receptor has a dynamic structure. Secondly, the resultant structures are stable over several hundred picoseconds of molecular dynamics. Thirdly, the partial agonist pindolol gives results intermediate between those of agonist and antagonist, and similar results are obtained when Arg^{83} and Lys^{267} are mutated to their neutral form. Finally, although the domain-swapping rearrangement will be fully discussed elsewhere,[77] it should be noted that the agonist-induced change in tilt angles for helices 5 and 6 would help to stabilize a domain-swapped dimer containing one agonist molecule. This would arise because both the helix packing angles at the 5−6 interface would be close to the ideal value of ∼20°. (For the partial agonist, this would be true only for one of the pairs of helices.)

Acknowledgment. We wish to acknowledge Dr. Robert Bywater for many helpful, enthusiastic comments on domain swapping and Dr. Gert Vriend for a copy of WHATIF. We are also grateful to Terry Lybrand for supplying coordinates of his receptor models. This research was supported by the EPSRC, Studentship Number 94309861, and the BBSRC, Grant Number B/06081.

Supporting Information Available: Structures of the receptor and complexes, sequence homology, and additional AMBER parameters not reported elsewhere[14] (9 pages). Ordering information is given on any current masthead page.

References

(1) Watkinson, S.; Arkinstall, S. *The G-protein linked receptor facts book*; Academic Press: London, 1994. Baldwin, J. M. Structure and function of receptors coupled to G-proteins. *Curr. Opin. Struct. Biol.* **1994**, *6*, 180−190.

(2) Strader, C. D.; Fong, T. M.; Tota, M. R.; Underwood, D. Structure and function of G-protein coupled receptors. *Annu. Rev. Biochem.* **1994**, *63*, 101−132.

(3) Timmermans, P. B. M. W. N.; Chui, A.; Hoolen, A.; Main, B. G. α-Adrenergic receptors. In *Comprehensive Medicinal Chemistry*; Emmett, J. C., Ed.; Pergamon: Oxford, 1990; Vol. 3, Chapter 12.1, 12.2, pp 133−187. Main, B. G. *β*-Adrenergic receptors. *Ibid*. Chapter 12.2, pp 188−228. Cooper, D. G.; Young, R. C.; Durant, G. J.; Ganellin, C. R. Histamine receptors. *Ibid*. Chapter 12.5, pp 323−422. Wess, J.; Buhl, T.; Lambrech, T. G.; Mutschler, E. Colinergic receptors. *Ibid*. Chapter 12.6, pp 423−492. Hibert, M.; Mir, A. K.; Fozand, J. R. Serotonin receptors. *Ibid*. Chapter 12.9, pp 567−600.

(4) Maggio, R.; Vogel, Z.; Wess, J. Reconstitution of functional muscarinic receptors by coexpression of amino-terminal and carboxyl-terminal receptor fragments. *FEBS Lett.* **1993**, *319*, 195−200. Kobilka, B. K.; Kobilka, T. S.; Daniel, K.; Regan, J. W.; Caron, M. G.; Lefkowitz, R. J. Chimeric alpha-2-adrenergic, beta-2-adrenergic receptors - delineation of domains involved in effector coupling and ligand-binding specificity. Science **1988**, *240*, 1310−1316.

(5) Maggio, R.; Vogel, Z.; Wess, J. Coexpression studies with mutant muscarinic adrenergic-receptors provide evidence for intermolecular cross-talk between G-protein-linked receptors. *Proc. Natl. Acad. Sci. U.S.A.* **1993**, *90*, 3103−3107.

(6) Luo, X.; Zhang, D.; Weinstein, H. Ligand-induced domain motion in the activation mechanism of a G-protein-coupled receptor. *Protein Eng.* **1994**, *7*, 1441−1448. Zhang, D.; Weinstein, H. Signal transduction by a 5-HT_2 receptor: A mechanistic Hypothesis from molecular dynamics simulations of the three-dimensional model of the receptor complexed to ligands. *J. Med. Chem.* **1993**, *36*, 934−938.

(7) Gether, U.; Lin, S.; Kobilka, B. K. Fluorescent labelling of purified β_2-adrenergic receptor. *J. Biol. Chem.* **1995**, *270*, 28268−28275.

(8) Farrens, D. L.; Altenbach, C.; Yang, K.; Hubbell, W. L.; Khorana, H. G. Requirement of rigid-body motion of transmembrane helices for light activation of rhodopsin. *Science* **1996**, *274*, 768−770.

(9) Gether, U.; Ballesteros, J. A.; Seifert, R.; Sanders-Bush, E.; Weinstein, H.; Kobilka, B. K. Structural instability of a constitutively active G protein-coupled receptor. *J. Biol. Chem.* **1997**, *272*, 2587−2590.

(10) Javitch, J. A.; Fu, D.; Liapakis, G.; Chen, J. Constitutive activation of the β_2 adrenergic receptor alters the orientation of its sixth membrane-spanning segment. *J. Biol. Chem.* **1997**, *272*, 18546−18549.

(11) Kyle, D. J.; Chakravarty S.; Sinsko, J. A.; Stormann, T. M. A proposed model of bradykinin bound to the rat B2 receptor and its utility for drug design. *J. Med. Chem.* **1994**, *37*, 1347−1354.

(12) Strader, C. D.; Sigal, I. S.; Register, R. B.; Candelore, W. S.; Rands, A.; Dixon, R. A. F. Identification of residues required for ligand binding to the beta adrenergic receptor. *Proc. Natl. Acad. Sci. U.S.A.* **1987**, *84*, 4384−4388. Strader, C. D.; Sigal, I. S.; Candelore, M. R.; Rands, E.; Hill, W. S.; Dixon, R. A. F. Conserved aspartic acid residues 79 and 113 of the beta adrenergic receptor have different roles in receptor function. *J. Biol. Chem.* **1988**, *263*, 10267−10271.

(13) Strader, C. D.; Candelore, M. R.; Hill, W. S.; Irving, I. S.; Dixon, R. A. F.; Sigal, I. S. Identification of two serine residues involved in agonist activation of the beta adrenergic receptor. *J. Biol. Chem.* **1989**, *264*, 13572−13578.

(14) Gouldson, P. R.; Winn, P. J.; Reynolds, C. A. A molecular dynamics approach to receptor mapping: application to the $5HT_3$ and β_2-adrenergic receptors. *J. Med. Chem.* **1995**, *38*, 4080−4086.

(15) Henderson, R.; Baldwin, J. M.; Ceska, T. A.; Zemlin, F.; Beckmann, E.; Downing, K. H. Model for the structure of bacteriorhodopsin based on high-resolution electron cryomicroscopy. *J. Mol. Biol.* **1990**, *213*, 899−929.

(16) Schertler, G. F. X.; Villa, C.; Henderson, R. Projection structure of rhodopsin. *Nature* **1993**, *362*, 770−772.

(17) Unger, V. M.; Schertler, G. F. X. Low resolution structure of bovine rhodopsin determined by electron cryo-microscopy. *Biophys. J.* **1995**, *68*, 1776−1786.

(18) Baldwin, J. M. The probable arrangement of the helices in G protein-coupled receptors. *EMBO J.* **1993**, *12*, 1693−1703.

(19) Herzyk, P.; Hubbard, R. E. Modeling of aminergic G-protein coupled receptors from experimental data by rule-based automated procedure. *Biophys. J.* **1996**, 70, p.mp169. Herzyk, P.; Hubbard, R. E. Automated-method for modelling 7-helix transmembrane receptors from experimental-data. *Biophys. J.* **1995**, *69*, 2419−2442.

(20) Rost, B. Predicting one-dimensional protein structure by profile based neural networks. *Methods Enzymol.* **1996**, *266*, 525−539.

(21) Altenbach, C.; Yang, K.; Farrens, D. L.; Farahbakhsh, Z. T.; Khorana, G.; Hubbell, W. L. Structural features and light-dependent changes in the cytoplasmic interhelical E-F loop region of rhodopsin: a site-directed spin-labeling study. *Biochemistry* **1996**, *35*, 12470−12478.

(22) Farahbakhsh, Z. T.; Ridge, K. D.; Khorana, H. G.; Hubbell, W. L. Mapping light-dependent structural changes in the cytoplasmic loop connecting helices C and D in rhodopsin: a site-directed spin labeling study. *Biochemistry* **1995**, *34*, 8812−8819.

(23) Vriend, G. WALIGN in WHATIF: A molecular modelling and drug design program. *J. Mol. Graph.* **1990**, *8*, 52−56.

(24) Suryanarayana, S.; Kobilka, B. K. Amino-acid Substitutions at position 312 in the 7th hydrophobic Segment of the beta(2)-adrenergic receptor modify ligand-binding specificity. *Mol. Pharmacol.* **1993**, *44*, 111−114. Suryanarayana, S.; Daunt, D. A.; von Zastrow, M.; Kobilka, B. K. A point mutation in the seventh hydrophobic domain of the α_2-adrenergic receptor increases its affinity for a family of β receptor antagonists. *J. Biol. Chem.* **1991**, *266*, 15488−15492.

(25) Liu, J.; Schöneberg, T.; van Rhee, M.; Wess, J. Mutational analysis of the relative orientation of transmembrane helices I and VII in G-protein coupled receptors. *J. Biol. Chem.* **1995**, *270*, 19532−19539.

(26) Gocayne, J. D.; Robinson, D. A.; Fitzgerald, M. G.; Chung, F. Z.; Kerlavage, A. R.; Lentes, K. U.; Lai, J.; Wang, C. D.; Fraser, C. M.; Venter, J. C. Primary structure of rat cardiac beta-adrenergic and muscarinic cholinergic receptors obtained by automated DNA sequence analysis. Further evidence for a multigene family. *Proc. Natl. Acad. Sci. U.S.A.* **1987**, *84*, 8296−8300.

(27) Zhou, W.; Flanagan, C.; Ballesteros, J. A.; Konvicka, K.; Davidson, J. S.; Weinstein, H.; Millar, R. P.; Sealfon, S. C. A reciprocal mutation supports helix-2 and helix-7 proximity in the gonadotropin-releasing-hormone receptor. *Mol. Pharmacol.* **1994**, *45*, 165−170. Sealfon, S. C.; Chi, L.; Ebersole, B. J.; Rodic, V.; Zhang, D.; Ballesteros, J. A.; Weinstein, H. Related contribution of specific helix-2 and helix-7 residues to conformational activation of the serotonin 5-HT_{2A} receptor. *J. Biol. Chem.* **1995**, *270*, 16683−16688.

(28) Vriend, G. WHATIF: A molecular modelling and drug design program. *J. Mol. Graph.* **1990**, *8*, 52−56.

(29) Weiner, S. J.; Kollman, P. A.; Case, D. A.; Singh, U. C.; Ghio, C.; Alagona, G.; Profeta, S., Jr.; Weiner, P. A new force field for molecular mechanics simulation of nucleic acids and proteins.

J. Am. Chem. Soc. **1984**, *106*, 765−784. Weiner, S. J.; Kollman, P. A.; Nguyen, D. T.; Case, D. A. An all atom force field for simulations of proteins and nucleic acids. *J. Comput. Chem.* **1986**, *7*, 230−252.

(30) Singh, U. C.; Weiner, P. K.; Caldwell, J. W.; Kollman, P. A. AMBER (Version 4.0); Department of Pharmaceutical Chemistry, University of California: San Francisco, CA, 1988.

(31) Dewar, M. J. S.; Zoebisch, E. G.; Healey, E. F.; Stewart, J. J. P. AM1: A new general purpose quantum mechanical molecular model. *J. Am. Chem. Soc.* **1985**, *107*, 3902−3909.

(32) Ferenczy, G. G.; Reynolds, C. A.; Richards, W. G. Semi-empirical AM1 electrostatic potentials and potential derived charges: A comparison with ab initio values. *J. Comput. Chem.* **1990**, *11*, 159−169.

(33) Reynolds, C. A.; Ferenczy, G. G.; Richards, W. G. Methods for determining the reliability of semiempirical electrostatic potentials and potential derived charges. *J. Mol. Struct. (Theochem)* **1992**, *256*, 249−269.

(34) Goodford, P. J. A computational procedure for determining energetically favorable binding sites on biologically important macromolecules. *J. Med. Chem.* **1985**, *28*, 849−857.

(35) Cheney, B. V.; Schulz, M. W.; Cheney, J.; Richards, W. G. Hydrogen-bonded complexes involving benzene as an H-acceptor. *J. Am. Chem. Soc.* **1988**, *110*, 4195−4198. Cheney, J.; Cheney, B. V.; Richards, W. G. Calculation of NH···π-hydrogen bond-energies in basic pancreatic trypsin-inhibitor. *Biochim. Biophys. Acta* **1988**, *954*, 137−139.

(36) Ferenczy, G. G.; Winn, P. J.; Reynolds, C. A. Towards improved force fields. II. Effective distributed multipoles. *J. Phys. Chem.* *101*, 5446−5455.

(37) Maloneyhuss, K.; Lybrand, T. P. 3-Dimensional structure for the β_2 adrenergic-receptor protein based on computer modeling studies. *J. Mol. Biol.* **1992**, *225*, 859−871.

(38) Gouldson, P. R.; Bywater, R. P.; Reynolds, C. A. A correlated mutation analysis of subtype specificity in the adrenergic, dopaminergic and muscarinic receptors. *Protein Sci.*, submitted for publication.

(39) Kontoyianni, M.; Deweese, C.; Penzotti, J. E.; Lybrand, T. P. 3-Dimensional models for agonist and antagonist complexes with β_2-adrenergic-receptor. *J. Med. Chem.* **1996**, *39*, 4406−4420.

(40) Adham, N.; Tamm, J. A.; Salon, J. A.; Vaysse, P. J. J.; Weinshank, R. L.; Branchek, T. A. A single-point mutation increases the affinity of serotonin 5-$HT_{1d-\alpha}$, 5-$HT_{1d-\beta}$, 5-HT_{1e} and 5-HT_{1f} receptors for β-adrenergic antagonists. *Neuropharmacology* **1994**, *33*, 387−391.

(41) Wess, J.; Maggio, R.; Palmer, J. R.; Vogel, Z. Role of conserved threonine and tyrosine residues in acetylcholine binding and muscarinic receptor activation. *J. Biol. Chem.* **1992**, *267*, 19313−19319.

(42) Wess, J.; Gdula, D.; Brann, M. R. Site-directed mutagenesis of the M_3 muscarinic receptor: identification of a series of threonine and tyrosine residues involved in agonist but not antagonist binding. *EMBO J.* **1991**, *10*, 3729−3734.

(43) Dahl, S. G.; Edvardsen, O.; Sylte, I. Molecular-dynamics of dopamine at the D_2 receptor. *Proc. Natl. Acad. Sci. U.S.A.* **1991**, *88*, 8111−8115.

(44) Mizobe, T.; Maze, M.; Lam, V.; Suryanarayana, S.; Kobilka, B. K. Arrangement of transmembrane domains in adrenergic receptors. *J. Biol. Chem.* **1996**, *271*, 2387−2389.

(45) Elling, C. E.; Schwartz, T. Connectivity and orientation of the seven helical bundle in the tachykinin NK-1 receptor probed by zinc site engineering. *EMBO J.* **1996**, *15*, 6213−6219.

(46) Smythe, M. L.; Huston, S. E.; Marshall, G. R. The molten helix - effects of solvation on the alpha-helical to 3_{10}-helical transition. *J. Am. Chem. Soc.* **1995**, *117*, 5445−5452.

(47) Huang, R.-R. C.; Yu, H.; Strader, C. D.; Fong, T. M. Interaction of substance-P with the 2nd and 7th transmembrane domains of the neurokinin-1 receptor. *Biochemistry* **1994**, *33*, 3007−3013.

(48) MacArthur, M. W.; Thornton, J. M. Influence of proline residues on protein conformation. *J. Mol. Biol.* **1991**, *218*, 397−412.

(49) Fu, D.; Ballesteros, J. A.; Weinstein, H.; Chen, J.; Javitch, J. A. Residues in the seventh membrane-spanning segment of the dopamine D2 receptor accessible in the binding-site crevice. *Biochemistry* **1996**, *35*, 11278−11285.

(50) Findlay, J. B. C.; Pappin, D. J. C. The opsin family of receptors. *Biochem. J.* **1986**, *238*, 625−642.

(51) Barlow, D. J.; Thornton, J. M. Helix geometry in proteins. *J. Mol. Biol.* **1988**, *201*, 601−619.

(52) Wong, S. K. F.; Slaughter, C.; Ruoho, A. E.; Ross, E. M. The catecholamine binding-site of the beta-adrenergic-receptor is formed by juxtaposed membrane-spanning domains. *J. Biol. Chem.* **1988**, *263*, 7925−7928.

(53) Wess, J.; Nanavati, S.; Vogel, Z.; Maggio, R. Functional role of proline and tryptophan residues highly conserved among G-protein coupled receptors studied by mutational analysis of the M_3 muscarinic receptor. *EMBO J.* **1993**, *12*, 331−338.

(54) Berlose, J. P.; Convert, O.; Brunissen, A.; Chassaing, G.; Lavielle, S. Three-dimensional structure of the highly conserved seventh transmembrane domain of G-protein-coupled receptors. *Eur. J. Biochem.* **1994**, *225*, 827−843.

(55) Barak, L. S.; Tiberi, M.; Freedman, N. J.; Kwatra, M. M.; Lefkowitz, R. J.; Caron, M. G. A highly conserved tyrosine residue in G-protein-coupled receptors is required for agonist-mediated beta(2)-adrenergic receptor sequestration. *J. Biol. Chem.* **1994**, *269*, 2790−2795.

(56) Javitch, J. A.; Fu, D. Y.; Chen, J. Y.; Karlin, A. Residues in the fifth membrane-spanning segment of the dopamine D2 receptor exposed in the binding-site crevice. *Biochemistry* **1995**, *34*, 16433−16439.

(57) Elling, C. E.; Nielsen, S. M.; Schwartz, T. W. Conversion of antagonist-binding site to metal-ion site in the neurokinin NK-1 receptor. Nature **1995**, *374*, 74−77.

(58) Thirstrup, K.; Elling, C. E.; Hjorth, S. A.; Schwartz, T. W. Construction of a high affinity zinc switch in the κ-opioid receptor. *J. Biol. Chem.* **1996**, *271*, 7875−7878.

(59) Sheikh, S. P.; Zvyaga, T. A.; Lichtarge, O.; Sakmar, T. P.; Bourne, H. R. Rhodopsin activation blocked by metal-ion-binding sites linking transmembrane helix-C and helix-F. *Nature* **1996**, *383*, 347−350.

(60) Javitch, J. A.; Fu, D.; Chen, J.; Karlin, A. Mapping the binding site crevice of the dopamine D2 receptor by the substituted cysteine accessibility method. *Neuron* **1995**, *14*, 825−831.

(61) Siebert, F. Probing the 7TM receptor activation by a combination of FT-IR spectrocopy and mutagenesis. Presented at the 661st Biochemical Society Meeting, Bath, United Kingdom, 1997.

(62) Higaki, J. N.; Fletterick, R. J.; Craik, C. S. Engineered metal-loregulation in enzymes. *TIBS* **1992**, *17*, 100−104.

(63) Kyte, J.; Doolittle, R. F. A simple method for displaying the hydropathic character of a protein. *J. Mol. Biol.* **1982**, *157*, 105−132.

(64) Chou, P. Y.; Fasman, G. D. Prediction of the secondary structure of proteins from their amino acid sequence. *Adv. Enzyml.* **1978**, *47*, 45−148.

(65) Donnelly, D.; Findlay, J. B. C.; Blundell, T. L. Human β_2-adrenergic model. *Receptors Channels* **1994**, *2*, 61−78.

(66) R. P. Bywater, Novo Nordisk A/S, DK-2880 Bagsvaerd, Denmark (unpublished coordinates deposited at the EMBL GPCR database; see following reference (http://www.sander.embl-heidelberg.de/7tm/)).

(67) Trumppkallmeyer, S.; Hoflack, J.; Bruinvels, A.; Hibert, M. Modeling of G-protein-coupled receptors - application to dopamine, adrenaline, serotonin, acetylcholine, and mammalian opsin receptors. *J. Med. Chem.* **1992**, *35*, 3448−3462.

(68) GPCRDB: Information system for G protein-coupled receptors (GPCRs), European Molecular Biology Laboratory, Heidelberg, Germany (http://www.sander.embl-heidelberg.de/7tm/).

(69) Blueml, K.; Mutschler, E.; Wess, J. Functional role in ligand binding and receptor activation of an arginine residue present in the sixth transmembrane domain of all muscarinic acetylcholine receptors. *J. Biol. Chem.* **1994**, *269*, 18870−18876.

(70) Kobilka, B. K.; Kobilka, T. S.; Daniel, K.; Regan, J. W.; Caron, M. G.; Lefkowitz, R. J. Chimeric α_2-adrenergic, β_2-adrenergic receptors - delineation of domains involved in effector coupling and ligand-binding specificity. *Science* **1988**, *240*, 1310−1316.

(71) Singer, M. S.; Oliveira, L.; Vriend, G.; Shepherd, G. M. Potential ligand binding residues in rat olfactory receptors identified by correlated mutation analysis. *Receptors Channels* **1995**, *3*, 89−95.

(72) Choudhary, M. S.; Sachs, N.; Uluer, A.; Glennon, R. A.; Westkaemper, R. B.; Roth, B. L. Differential ergoline and ergopeptine binding to 5-hydroxytryptamine$_{2A}$ receptors: Ergolones require an aromatic residue at position 340 for high affinity binding. *Mol. Pharmacol.* **1995**, *47*, 450−457.

(73) Kontoyianni, M.; Lybrand, T. P. Computer modelling studies of G-protein coupled receptors. *Med. Chem. Res.* **1993**, *3*, 407−418.

(74) Gouldson, P. R.; Reynolds, C. A. Simulations on dimeric peptides: evidence for domain swapping in G-protein coupled receptors? *Biochem. Soc. Trans.* **1997**, *25*, 1066−1071.

(75) Liu, J.; Blin, N.; Conklin, B. R.; Wess, J. Molecular mechanisms involved in muscarinic acetylcholine receptor-mediated G-Protein activation studied by insertion mutagenesis. *J. Biol. Chem.* **1996**, *271*, 6172−6178. Bluml, K.; Mutschler, E.; Wess, J. Insertion mutagenesis as a tool to predict the secondary structure of a muscarinic receptor domain determining specificity of G-protein coupling. *Proc. Natl. Acad. Sci. U.S.A.* **1994**, *91*, 7980−7984.

(76) Wilson, A. L.; Guyer, C. A.; Cragoe, E. J.; Limbird, L. E. The hydrophobic tryptic core of the porcine alpha-2-adrenergic receptor retains allosteric modulation of binding by Na+, H+, and 5-amino-substituted amiloride analogs. *J. Biol. Chem.* **1990**, *265*, 17318−17322.

(77) Gouldson, P. R.; Snell, C. R.; Bywater, R. P.; Reynolds, C. A. Domain swapping: a possible mechanism for functional rescue and activation in G-protein coupled receptors. *Protein Eng.*, submitted for publication.

(78) Bennett, M. J.; Schlunegger, M. P.; Eisenberg, D. 3D Domain swapping: A mechanism for oligomer assembly. *Protein Sci.* **1995**, *4*, 2455−2468.

(79) Tegoni, M.; Ramoni, R.; Bignetti, E.; Spinelli, S.; Cambillau, C. Domain swapping creates a 3rd putative combining site in bovine odorant binding-protein dimer. *Nature Struct. Biol.* **1996**, *3*, 863−867.
(80) Maggio, R.; Barbier, P.; Fornai, F.; Corsini, G. U. Functional-role of the 3rd cytoplasmic loop in muscarinic receptor dimerization. *J. Biol. Chem.* **1996**, *271*, 31055−31060.
(81) Hebert, T. E.; Moffett, S.; Morello, J.-P.; Loisel, T. P.; Bichet, D. G.; Barret, C.; Bouvier, M. A peptide derived from a β_2-adrenergic receptor transmembrane domain inhibits both receptor dimerisation and activation. *J. Biol. Chem.* **1996**, *271*, 16384−16392.
(82) Ng, G. Y. K.; O'Dowd, B. F.; Lee, S. P.; Chung, H. T.; Brann, M. R.; Seeman, P.; George, S. R. Dopamine d2 receptor dimers and receptor-blocking peptides. *Biochem. Biophys. Res. Commun.* **1996**, *227*, 200−204.
(83) Schöneberg, T.; Liu, J.; Wess, J. Plasma-membrane localisation and functional rescue of truncated forms of a G-protein-coupled receptor. *J. Biol. Chem.* **1995**, *270*, 18000−18006.
(84) Ridge, K. D.; Lee, S. S. J.; Abdulaev, N. G. Examining rhodopsin folding and assembly through expression of polypeptide fragments. *J. Biol. Chem.* **1996**, *271*, 7860−7867.
(85) Gudermann, T.; Schöneberg, T.; Schultz, G. Functional and structural complexity of signal transduction via G-protein coupled receptors. *Annu. Rev. Neurosci.* **1997**, *20*, 399−427.
(86) Monnot, C.; Bihoreau, C.; Conchon, S.; Curnow, K. M.; Corvol, P.; Clauser, E. Polar residues in the transmembrane domains of the type-1 angiotensin-II receptor are required for binding and coupling - reconstitution of the binding-site by coexpression of 2 deficient mutants. *J. Biol. Chem.* **1996**, *271*, 1507−1513.
(87) Jarv, J. A model of nonexclusive binding of agonist and antagonist on G-protein coupled receptors. *J. Theoret. Biol.* **1995**, *175*, 577−582.
(88) De Meyts, P.; Ursø, B.; Christoffersen, C. T.; Shymko, R. M. Mechanism of insulin and IGF-I receptor activation and signal transduction specificity. *Ann. N. Y. Acad. Sci.* **1995**, *766*, 388−401.
(89) Samama, P.; Cotecchia, S.; Tommaso, C.; Lefkowitz, R. A. mutation-induced activated state of the beta-2-adrenergic receptor. *J. Biol. Chem.* **1993**, *268*, 4625−4636.
(90) Surprenant, A.; Horstman, D. A.; Akbarali, H.; Limbird, L. E. A point mutation of the alpha-2-adrenoceptor that blocks coupling to potassium but not calcium currents. *Science* **1992**, *257*, 977−980.
(91) Kaushal, S.; Korana, H. G. Structure and function in rhodopsin VII. Point mutations associated with autosomal dominant retinis pigmentosa. *Biochemistry* **1994**, *33*, 6121−6128.
(92) Rao, V. R.; Cohen, G. B.; Oprian, D. D. Rhodopsin mutation G90D and a molecular mechanism for congenital night blindness. *Nature* **1994**, *367*, 639−642.
(93) Nakayama, T. A.; Korana, H. G. Mapping of the amino acids in the membrane-embedded helices that interact with the retinal chromaphore in bovine rhodopsin. *J. Biol. Chem.* **1990**, *266*, 4269−4275.
(94) Oliveira, L.; Paiva, A. C.; Vriend, G. A common motif in G-protein coupled seven transmembrane helix receptors. *J. Comput.-Aided Mol. Des.* **1993**, *7*, 649−658.
(95) Neitz, M.; Neitz, J.; Jacobs, G. H. Spectral tuning of pigments underlying red green color vision. *Science* **1991**, *252*, 971−974.
(96) Oprian, D. D. The ligand-binding domain of rhodopsin and other G-protein-linked receptors. *J. Bioenerg. Biomembr.* **1992**, *24*, 211−217.
(97) Ridge, K. D.; Bhattacharya, S.; Nakayama, T. A.; Korana, H. G. Light stable rhodopsin. II. An opsin mutant (Trp-265-Phe) and a retinal analog with an isomerizable 11-cis configuration form a photostable chromaphore. *J. Biol. Chem.* **1992**, *267*, 6770−6775.
(98) Dryja, T. P.; Berson, E. L., Rao, V. R.; Oprian, D. D. Heterozyqous missense mutation in the rhodopsin gene as a cause of gongential stationary night blindness. *Nat. Genet.* **1993**, *4*, 280−283.
(99) O'Dowd, B. F.; Hantowich, M.; Regan, J. W.; Leader, W. M.; Caron, M. G.; Lefkowitz, R. Site-directed mutagenesis of the cytoplasmic domains of the human beta-2-adrenergic receptor - localisation of regions involved in G-protein-receptor coupling. *J. Biol. Chem.* **1988**, 263, 15985−15992.
(100) Wang, H. Y.; Lipfert, L.; Malbon, C. C.; Bahouth, S. Site-directed anti-peptide antibodies define the topography of the beta-adrenergic-receptor. *J. Biol. Chem.* **1989**, *264*, 14421−14431.
(101) Fraser, C. M.; Chung, F. Z.; Wang, C. D.; Venter, J. C. Site-directed mutagenesis of human beta-adrenergic receptors - substitution of aspartic acid-130 by asparagine produces a receptor with high-affinity agonist binding that is uncoupled from adenylate-cyclase. *Proc. Natl. Acad. Sci. U.S.A.* **1988**, *85*, 5478−5482.
(102) Fraser, C. M. Site-Directed Mutagenesis of Beta-adrenergic receptors - identification of conserved cysteine residues that independently affect ligand-binding and receptor activation. *J. Biol. Chem.* **1989**, *264*, 9268−9270.
(103) Valiquette, M.; Bonin, H.; Bouvier, M. Mutation of tyrosine-350 impairs the coupling of the beta-2-adrenergic receptor to the stimulatory guanine-nucleotide-binding protein without interfering with receptor downregulation. *Biochemistry* **1993**, *32*, 4979−4985.

JM960647N